NOVEL PEPTIDE-BASED MATERIALS ASSEMBLE INTO ADHESIVE STRUCTURES: CIRCULAR DICHROISM, INFRARED SPECTROSCOPY, AND TRANSMISSION ELECTON MICROSCOPY STUDIES

by

MATTHEW D. WARNER

B.S., Kansas State University, 2006

A THESIS

submitted in partial fulfillment of the requirements for the degree

MASTER OF SCIENCE

Department of Biochemistry
College of Arts and Sciences

KANSAS STATE UNIVERSITY
Manhattan, Kansas

2009

Approved by:

Major Professor
John. M. Tomich

Abstract

Biologically based adhesives offer many industrial advantages over their chemically synthesized counterparts, not the least of which are reduced environmental impact and limited toxicity. They also represent a renewable resource. In addition, nanoscale biomaterials also show an incredibly large potential for biomedical uses, including possible drug delivery and novel wound bandaging, as well as tissue engineering. Understanding the adhesion mechanisms at work in peptide-based nanomaterials is key for producing viable industrial and clinical bio-mimetic compounds. Our previous work has shown that small hydrophobic oligopeptide segments flanked by short tri-lysine sequences display adhesion strength that is dependent on the formation of β-structure and large-scale association of monomers. In this study, three oligopeptides were synthesized based on putative amyloid fibril nucleation sites. Two of the sequences originate from the Alzheimer's beta amyloid peptide $A\beta_{1\text{-}40}$, while the third sequence comes from a nucleation site for islet amyloid polypeptide (IAPP). These peptides show unusual structural properties associated with adhesive ability. Furthermore, they represent a third category of requirements for β-structure formation. In addition, I report the first morphological evidence for the previously predicted structural mechanism underlying our previous peptide-based adhesives.

Table of Contents

List of Abbreviations

θ	Observed ellipticity, mdeg.
[θ]	Mean residue ellipticity, deg. cm^2 $decimole^{-1}$
Aβ	Alzheimer's beta-amyloid peptide
$Aβ_{16-21}$	Hydrophobic sequence KLVFFA, or KKKLVFFAKKK
$Aβ_{30-35}$	Hydrophobic sequence AIIGLM, or KKKAIIGLMKKK
CD	Circular dichroism
DHP	Dihydropyridine
DI	Deionized, distilled water
DOPA	3,4-dihydroxy-phenylalanine
EM	Electron microscope
FT-IR, IR	Fourier transform infrared spectroscopy
h	Hydrophobic sequence FLIVIGSII
h_{5n}	Hydrophobic sequence FLIVI
h_{5c}	Hydrophobic sequence IGSII
h_{5mI}	Hydrophobic sequence IVIGS
HPLC	High performance liquid chromatography
$IAPP_{23-28}$	Islet amyloid polypeptide, or the hydrophobic sequences IFGAIL, or KKKIFGAILKKK
TEM	Transmission electron microscopy (or micrograph)
TFA	Trifluoroacetic acid

List of Figures

List of Tables

Acknowledgments

I owe many people a debt of gratitude for the patience and kindness with which they treated me. To Dr. Om Prakash and Dr Gerald Reeck, committee members and two of my favorite teachers, who have shown me untold kindness by teaching and advising me over the years, for putting up with my absentmindedness, and without whom this degree would be impossible. To Pinakin Sukthankar, the fastest friend I've ever made, for allowing me to get to know him. I hope I may have the privilege for many years to come. To Dr. Takeo Iwamoto, for helping me when I needed it, for always being patient, no matter how annoying I'm sure I must have become, and for reassuring me by his presence that there are still a few Renaissance men left in the world. To Sushanth Gudlur for helping me when I needed someone to cover my experiments at the lab over absences and for aiding with instrumentation problems. To Nozomi Matsumiya for great conversations and fun in the lab. To God, for everything, literally. Thank you to the wonderful KSU Biochemistry Department, faculty, and staff for their help and guidance, and for making my days a bit brighter.

Dedication

It is fair to say in a very literal sense that I would not be here if it were not for Dr. Tomich. I ultimately decided to attend K-State after speaking with him about biochemistry and the university. It is, in fact, due in very large part to my conversation with him that I finally decided to pursue a career in biochemistry. Had I never met him, my life would be entirely different without that pivotal conversation, and I an entirely different person—and I fear that I would have missed out on a collegiate experience that has granted me more happiness, more friends, and more varied experiences than I could ever have expected or hoped for. In addition to deciding to come to KSU, that conversation piqued my interest in cystic fibrosis, Alzheimer's, and protein science that spurred my desire to work in his lab as an undergraduate. He has always had sage words for my situation, and always been ready to either encourage me or kick me in the pants, as the situation required. Both have been greatly valued, though I confess that I think encouraging words are easier to appreciate at the time they are spoken. However, as is usually the case, hard words are often more valuable than gold when spoken with caring intent, and Dr. Tomich has without doubt demonstrated this. He has been patient through very numerous mistakes on my part over the years and has helped me learn how to learn, and how to think. He also has shown me what shortcomings I need to improve on and conquer in order to be a good scientist. And these things are the most valuable to me. I cannot express my gratitude enough for all he has done for me over the years. Thanks for putting up with me!

I also wish to dedicate this work to my family, my mother, father, brother, and also to my good friends of many years ago, who were once and still remain my second family even though I have not spoken to some of them in many years. deMauri Mackie, Kristin White, Shannon Sanderson, Eric Skoglund, Andy Hyland, Tom Keegan, Mike Shults. They helped me though

the hardest times of my life and it is quite sure that without them I would have given up long ago. Words cannot express the depth of my gratitude to them for shaping my life and my character the way they have. It is impossible to articulate my unreserved love for these people who cared for me when I could not care for myself. They remain always in my prayers. My failures are my own, but it is certain that my successes belong as much to them as they do to me. Without them, I am nothing. There is no higher honor for me than to have known them.

To Dan Ratzlaff, who I consider a second brother, and who finally helped me out of my shell. By force when needed.

To Kyle Chapman, Chris Shipley, and Tim Bennett for teaching me the value of life through death. I miss you guys.

CHAPTER 1 - Introduction and Background to Biological Adhesives

Historical Perspective.

The use of adhesives for industrial applications is commonplace today. Adhesive development and manufacturing is a multi-billion dollar industry with marketed applications from high-grade construction bonding agents used in plywood fabrication and housing structures, to furniture construction, to mundane uses such as paper crafts and grade school projects. Specialized glues work in underwater applications and boating uses, and the construction of orchestral instruments. Though the big business aspects of adhesive development and marketing are relatively new, mankind's use of adhesives can be traced back more than 5 millennia. In fact, non-biological glues and sealants, despite having the dominant market share of high-end industrial and construction uses today, occupy only a tiny and recent addition in the overall history of glues. These agents are outside the scope of the present study, and therefore will not be discussed in detail. There is a large amount of research and literature on synthetic polymers that is best examined in other sources.

For more than 10,000 years man has employed glues and the resulting composites obtained from natural sources originating from an animal, plant, or mineral basis (Täljsten 2006, Delmonte 1989). One of the first known instances comes from prehistoric burial grounds, where broken pottery was found repaired with tree sap circa 4,000 B.C. (Täljsten 2006). The Babylonians created a tar-like adhesive to hold ivory pieces in temple decorations (Braude 1943, cited in Keimel 2003), and later the Egyptians would use animal derived glue for many furnishings found in the tombs of various pharaohs (Keimel 2003). The Egyptians also developed the one of the earliest procedures for making animal glue. It was used, among other

applications, for the making of bows (ibid.). Uses steadily multiplied for the various glues, but the resources for making them remained purely natural until very recently.

Only in the last 100 years have synthetic polymers been explored and developed, with the majority of the industrial interest since 1950 (Keimel 2003). Part of the reason for the dramatic rise in popularity of synthetic polymers was the ability to formulate different specific compounds for different specific purposes or materials. Part of the reason was also a dramatic increase in adhesion strength to weight ratios found with synthetics; this was key for aerospace engineering (ibid.). Finally, the decline in natural adhesive research can be seen to lie in part with the enormous assortment of biological sources. The immense diversity of organismal mechanisms for adhesion, combined with a technological inability to analyze the specific structure/function relationships led to a decline in research. Even now, with vastly advanced analytical instrumentation, the difficulties associated with determining individual components of biological glues are daunting.

General Adhesive Mechanisms.

Adhesives may be more appropriately called glues, as strictly speaking both adhesion and cohesion are required for a functioning "adhesive" or glue. Adhesion forces exist between a molecule or polymer and a substrate surface, such as a metal or wood joint, a rock, or various organic surfaces such as the plant leaves. Cohesion forces exist between individual monomers or polymers of a glue matrix. In order to be biologically or industrially useful, adhesives must be able to form attractive or mechanical interactions to desired bonding surfaces, as well as a cohesive structure stable enough to effectively fill and strengthen the interstitial gap between joints or surfaces.

Organisms most often use a combination of chemical, mechanical, and dispersive mechanisms to achieve their adhesion goals. Covalent chemical bonding with the substrate surface is not generally seen; however, organisms very commonly use covalent cross-linking as a means to achieve cohesion and modify properties such as elasticity within the adherent complexes themselves. This is often done employing different 3,4-dihydroxy phenylalanine (DOPA) chemistries (Wiegemann 2005). A primary example is the bonding system of the mussel *Myetilus edulis*, which uses DOPA as a crosslinking agent in the stiff outer protein that coats anchoring plaques, as well as the byssal threads connecting the mussel to its substrate surface (Waite 1983, Haemers *et al.* 2005, Wiegemann 2005, Silverman and Roberto 2007. See Figure 3). This coating encases a different kind of polymeric mix that has a more elastic quality.

Mechanical adhesives work primarily by filling the crevices, pores, or spaces of a surface and bond the surfaces by interlocking. Velcro is a widely used mechanical adhesive in the macroscopic world for shoes and fabrics. Other compounds may form a mechanical bond on microscopic or macromolecular scale. This form of adhesion should be contrasted with chemical or dispersive adhesion systems where bonding strength comes primarily from covalent linkage or van der Waal and London interactions, respectively. Aggregate fibril or filament-like protein structure is a preferred way for many bio-glues to entangle and interlock with various substrates. Fibril formation is also a common pathology in various disease processes. Cells may be entangled with plaques of fibrils, cutting them off from the surroundings as in Alzheimer's, for example (reviewed in Winklhofer *et al.* 2008).

Mechanical adhesion can also be illustrated by looking at a spool of thread: the whole spool consists of one continuous thread. However, examining the thread under a microscope at high magnification reveals that it is made of many small fibers that tangle together to form a

large aggregate thread. In the same way, mechanical adhesion entangles a surface by engaging small voids, crevices and pores. Although van der Waals/London forces may be significant as well, the hallmark of mechanical systems remains entanglement or interlocking interaction between adhesive and surface.

Biological systems use dispersive anchoring systems extensively as well—barnacle cement has both mechanical (filamentous/mesh-like microscopic structure) and dispersive aspects (reviewed in Wiegemann 2005). Both mussels and geckos use dispersion, with the gecko being a good example of "purely" dispersive adhesion—there is no protein or mucus secreted at all, and the interactions leading to adhesion are strictly van der Waals/London forces from structural adaptations on the gecko's feet (Autumn *et al.* 2002).

Organismal Adhesives.

There are a great number of organisms that use adhesive systems to attach themselves to anchor points, substrates, or other even organisms. These organisms range from microbes and fungi, to algae, to kelp, to mussels, crustaceans, and gastropods, to reptiles and amphibians such as the gecko and numerous frogs, respectively. A very brief overview of several of the different biological systems is useful for gaining an overall picture of bioadhesive research.

Adhesion in fungi serves many different purposes. Fungal adhesion prevents a separation from its preferred environment (Epstein and Nicholson 1997) by wind or water, facilitates penetration of the host tissue, and increases the ability to chemically interact with the host (Bechinger *et al.* 1999, Howard *et al.* 1991, Jones and Epstein 1990). It has been shown that the adhesive complex is liquid when secreted and subsequently polymerizes into a cross-linked compound with a fibrous appearance (Caesar-TonThat and Epstein 1991, Watanabe *et al.* 2000).

It has also been shown that the hydrophobicity of the substrate surface is a key factor in determining bonding strength (Epstein and Nicholson 1997). Unfortunately, there has not been much progress in the compositional analysis of fungal glue components, as the specific identification of individual compounds has largely eluded researchers. The cell surface of fungi is crowded and complex, and a large number of the biomolecules on the surface are cross-linked. This makes it even more difficult to identify individual glue components. Currently, it is known that components of fungal glues contain carbohydrates. In addition, these components must be secreted initially in a water-soluble composition, because in both aquatic and many types of terrestrial fungi, free water is required for germination. Glue components must thus be able to spread effectively in an aqueous environment.

Similarly to fungal species, algae utilize another adhesive system that has proven extremely difficult to characterize. In chapter six of Biological Adhesives, which covers marine brown algae, contributors Philippe Potin and Catherine Leblanc note that as late as 1998 "studies on adhesion mechanisms of marine brown algal adhesives have consisted mostly of analogy and hypothesis". They also note, citing a series of studies, that as late as 2002 most of the compositional analysis of algal systems was "circumstantial and based on methodologies such as histochemistry". Part of the reason for the lack of component determination may be the difficulty of isolating adhesive compounds from other algal extracellular polymers, such as the numerous polysaccharides present (Waite and Qin 2001, Mostaert *et al.* 2006). As with fungi, the cell surface is complex. In addition, the biological need for an adhesive complex that can bond to many different surfaces means the adhesive complex itself is highly heterogeneous; this also makes it difficult to separate the components for independent analysis.

Mussel and Barnacle Mechanisms.

Blue mussels (*Mytilus edulis*) contain one of the most extensively studied bioadhesive systems, and along with the barnacle represent the organisms studied with the most industrial interest. As a result, much more is known about the compositional elements and mechanism of anchoring in these systems than that of microorganisms or fungal and algal complexes. Mussels attach themselves to substrata through sticky plaques that link to threads comprised of collagen and a cured proteinaceous adhesive. These threads in turn connect to the stem at the base of the mussel's foot (Figure 1-1). Together the plaque and the threads form the byssus. A groove in the bottom of the foot organ called the byssal groove houses the glands that secrete the thread proteins. The proteins are mixed in the groove, in a manner analogous to injection molding, and then secreted. So far, 10 glue-related proteins have been isolated from *Mytilus edulis* (Silverman and Roberto 2007). The first protein to be isolated, *Mytilus edulis* foot protein 1 (Mefp-1), has been demonstrated to effectively bond to many different surfaces, including glass and Teflon (Figure 1-2). Because of this, it has received much commercial interest.

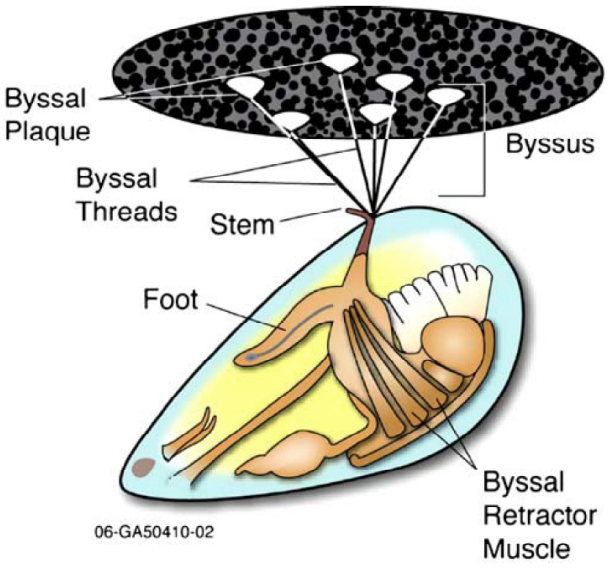

Figure 1-1. Mussel anatomy. Figure from Silverman and Roberto 2007.

Figure 1-2. Mussel attached to Teflon. Figure taken from the Wilker group web page. http://www.chem.purdue.edu/wilker/research/adhesives/onteflon35.jpg

Figure 1-3 shows the rough localization of glue proteins in the byssus. Each thread consists of an inner core that is collagenous and elastic, and an outer covering of Mefp-1, which is a relatively stiff polyphenolic protein with a 10-15% DOPA concentration (Waite 1983). DOPA cross-linking gives the byssal threads a relatively stiff cohesive strength. Mefp-1 does not conform to a solid secondary structure, instead existing in a random coil conformation with short helix-like segments repeatedly interspersed (Haemers *et al.* 2005). These helix-like sequences are made up of highly modified decapeptide repeats that contain DOPA and hydroxylated prolines. Almost 70% of amino acids are hydroxylated. (Silverman and Roberto 2007).

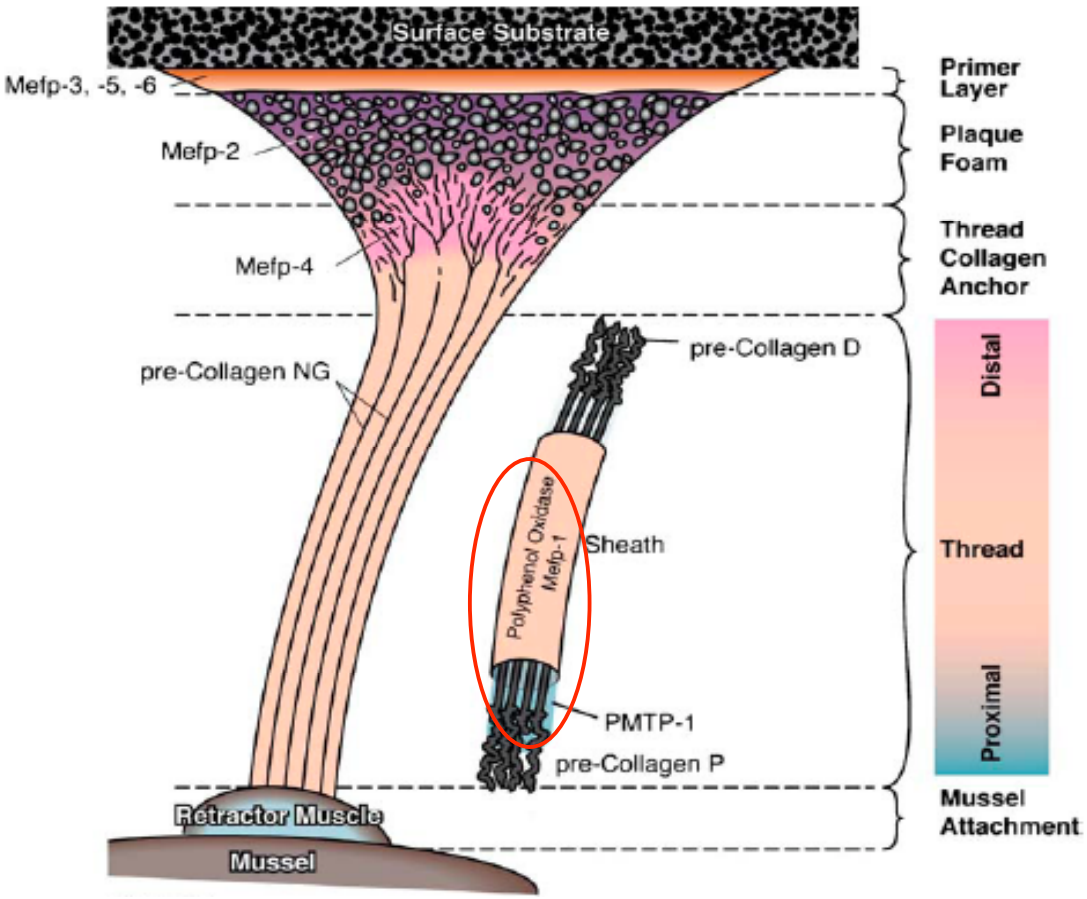

Figure 1-3. Proteins involved in byssal threads and plaques. Figure from Silverman and Roberto 2007. Mefp-1 comprises the byssal sheath over pre-Collagen fibers (circled in red).

The extended conformation is thought to contribute to Mefp-1's function by allowing the numerous hydroxylated groups to interact extensively with a variety of other proteins and surfaces. Mefp-3 and mefp-5 both have larger percentages of DOPA than mefp-1 (Papov *et al.* 1995, Waite and Qin 2001). However, the DOPA present in these two proteins is thought to be involved heavily in hydrogen bonding and non-covalent interactions, not cross-linking as in the outer coat of mefp-1. In addition, DOPA residues are able to complex with metal ions commonly present in mineral surfaces (Wiegemann 2005). The exact molecular mechanisms through which these various proteins interact with each other have yet to be determined, and are objects of current research.

Another relatively well-studied marine glue system is that of various barnacle species. Most research has been done on acorn barnacles, and therefore will be referred to from now on simply as barnacles. Barnacles undergo several stages of development before they reach the stage where permanent attachment is sought. These early stages are mobile. During the last stage before adulthood, the barnacle seeks a suitable surface for anchoring. This stage of development is known as the cypris stage, and the organism will secrete a small amount of strong cement to anchor itself and undergo transformation to an adult barnacle. Once it has undergone this transformation its sessile life begins, and it will begin to secrete adult cement. The cement glands secrete the adhesive mix through ducts and onto the surface through small gaps in the barnacle base plate. After the cement is cured, the collecting ducts are blocked off and unable to secrete any further adhesive. As the barnacle grows more ducts are developed at the edge of the base plate, and more cement is secreted (Figure 1-4).

Like mussel adhesive components, the barnacle cement is about 90% protein, with the remainder containing ash, lipid, and carbohydrates (Walker 1999). In contrast to mussel

adhesive, however, this cement mix does not rely on DOPA chemistry. Post-translational modifications and sequences of subunits constituting this system have no similarity to that of mussels either (Waite and Qin 2001). Instead, the barnacle secretion includes a combination of proteins of variable size, which contain many cysteine-rich repeats through which they may aggregate and crosslink to form high molecular weight cement (Naldrett and Kaplan 1997, Kamino *et al.* 2000, Kamino 2001, Nakano *et al.* 2007).

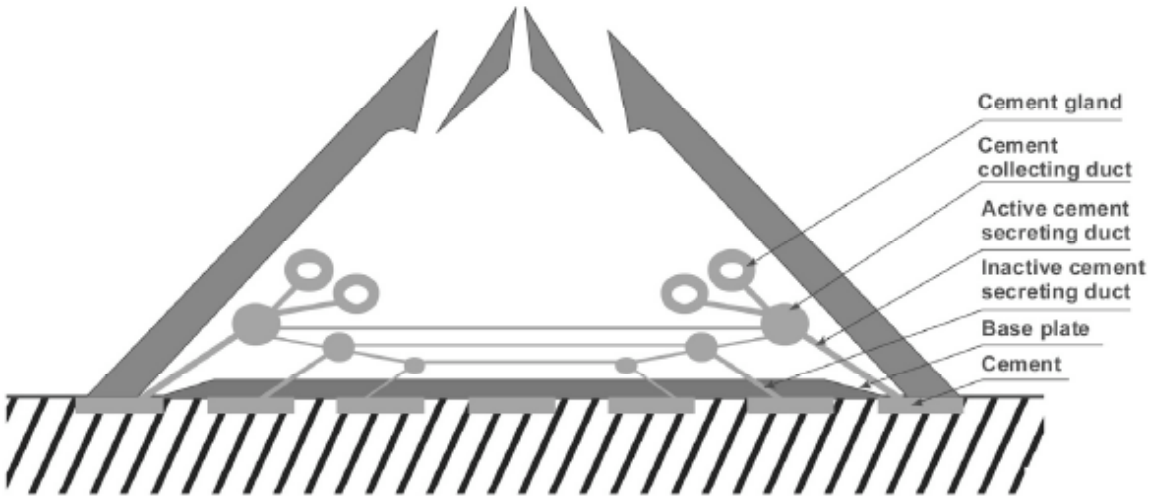

Figure 1-4. Barnacle anatomy. Taken from Wiegemann

An important characteristic of the protein aggregate in barnacle cement is the ability to change structurally to adapt to the surface potential of various substrates. Barnacles adhere to both polar and non-polar surfaces. When attached to polar surfaces, the proteins form a thin sheet with globular, mesh-like microstructure (Wiegemann and Waterman 2003). However, when attaching to non-polar surfaces, the proteins instead form filament-like structures that seem to be more elastic and extended (ibid.). In other words, its microstructure is adaptable to different environmental cues. Wiegemann reports that although shear strength of the cement suffers with a hydrophobic surface, its peel strength is enhanced (Wiegemann 2005).

Amyloid Pathology and Formation.

Fibrous protein aggregation is a major cause of pathologies in humans, as well as other organisms. Formation of fibrils can be driven by polymerization via cross-linking as seen in organisms such as various fungi and mussels, discussed above (Watanabe *et al.* 2000, Waite 1983, Silverman and Roberto 2007), or non-covalent aggregation as seen with Alzheimer's disease. The aggregation of beta amyloid protein is believed by many to be a cause of pathology in Alzheimer's. However, where it was once thought that only a few proteins could form amyloid fibrils, it has become clear that many proteins have this ability (Guijarro *et al.* 1998, Stefani and Dobson 2003, Uversky and Fink 2004, reviewed in Monsellier and Chiti 2007). In recent years, more instances of pathological fibril aggregation have been discovered. In one study, the authors examine the possibility that this potential for aggregation is a generic quality of most proteins and represents an evolutionary "driving force" (Monsellier and Chiti 2007).

Much of the current research on fibril formation has concentrated on amyloid-like behavior and inducible self-assembly with various conditions. The exact mechanisms behind amyloid formation are not yet understood, and as a result current work is looking for factors that alter or create fibrillar structures, with an end goal of material manipulation or pathological amyloid inhibition. Additionally, an interest in mimicking the microscopic structure of biological adhesives, especially the fibrillar mesh of barnacle cement, is widespread in current research. It was shown that peptides synthesized from repetitive sequence elements of the *Megabalanus rosa* barnacle protein can be made to self assemble in the presence of salt (Nakano *et al.* 2007). The self-assembly process is dependent on the presence of a salt concentration in the 1 M range. The assembled peptide also showed a mesh-like structure similar to native barnacle cement protein micrographs.

A number of laboratories are studying peptide nanomaterials related to amyloid fibrils. One group used short sequence fragments from β-sheet regions of the $A\beta_{1-40}$ peptide to look for nucleation sites that increased the aggregative ability of Aβ. They found that two sequences from residues 16-20 and 30-35 both accelerated aggregation (Liu *et al.* 2004). Another group looked at regions of islet amyloid polypeptide (IAPP) for nucleation sites and subsequently found a peptide containing residues from a hydrophobic turn sequence of IAPP had an ability to induce aggregation (Azriel and Gazit 2001). In 2001, Azriel and Gazit proposed that aromatic stacking played a role in the generation of amyloid fibrils. This was based on the results of previous work and the presence of aromatic residues in many other amyloid-related sequences (Azriel and Gazit 2001, Gazit 2002). However, although aromatic stacking may contribute to the energy requirement for fibril formation, it was shown to be insufficient by itself for aggregation (Tjernberg *et al.* 2002).

In addition to the almost ubiquitous ability of globular proteins to transform into amyloid fibrils and the discovery of nucleating molecules and sequences, much has been learned in the past decade about the nature of amyloid structure and aggregation. However, there still remain many unanswered questions concerning the specific mechanisms of fibril formation and the specific reasons behind cytotoxicity.

A number of models of amyloid self-assembly have been proposed and refined throughout the past decade. However, the specific molecular actions that take place during fibril formation are not well understood. This is largely due to the complexity of the assembly process. Great headway has also been made in assigning amyloid intermediates to on-pathway or off-pathway fibril formation processes (reviewed in Jahn and Radford 2008). Further, it is now known that the relative abundance of end-states in protein aggregation (amorphous

aggregates, worm-like fibrils, or long straight fibrils) varies according to pH, protein sequence and concentration, physical agitation of the solution, and ionic strength (Jahn and Radford 2008).

Amyloid formation is generally accepted to occur via a nucleated polymerization pathway. This process is a two-step process. The first phase is termed the "lag phase" and is characterized by little or no observable change in fibril concentration. The lag phase is considered the time needed for nuclei to form and is the rate-limiting step in fibril formation. A shorter lag phase corresponds to a smaller fibril concentration dependence on nuclei formation, and thus a smaller "critical nuclei". The lag phase may be significantly shortened or even eliminated by addition of nucleating species to a solution (Xue *et al.* 2008). In addition, absence of an observed lag phase does not necessarily indicate that fibril formation does not proceed via nucleation (Chiti and Dobson 2006). It may simply be that nucleus formation is not the rate-limiting step in the polymerization process. Formation of the nucleus is not thermodynamically favored (Jahn and Radford 2008). The second phase, called the "elongation phase", is characterized by mass conversion of protein to fibers via stacking or elongation of nuclei into mature fibrils. This step is much faster and is thermodynamically favored.

The identity of the nucleating species itself is an outstanding question. A large number of studies show a small concentration dependence of lag phase, and conclude that nucleating species is either very small or monomeric. However, evidence suggests the approach used for some of these studies is insufficient, and furthermore that it may skew the results of studies toward a small nucleation species (Xue *et al.* 2008). This is because conditions affecting the relative abundance of the end-state of aggregation (for example, amorphous aggregate vs. long straight fibrils, discussed above) can also affect the length of the lag phase. One such condition is mechanical agitation of the experimental solution (Nielsen *et al.* 2001, Xue *et al.* 2008)

Amyloid fibrils have several properties in common with synthetic polymers, and can be seen as a subset of polymer chemistry (nicely reviewed in Wetzel *et al.* 2007). The plasticity of amyloid fibrils, that is, the ability of amyloid to deform and reform, along with structural polymorphism, and the difficulties of inhibiting fibril growth, is an area where polymer chemistry perspectives, such as those created and refined in adhesive and plastics industry, can be extraordinarily helpful for biochemical amyloid fibril research. On the other hand, understanding the biological mechanisms and structures displaying adhesive properties can also shed light on questions central to amyloid assembly and pathology.

The readiness with which amyloid fibrils adopt alternative packing arrangements in adaptation to different stresses or sequence mutations is indicative of large structural degeneracy and is very similar to the ability of polymers to shift packing arrangements, but almost never seen in globular proteins (Wetzel *et al.* 2007). The authors hypothesize that the almost universal ability of proteins to undergo amyloid transformation is perhaps due to the polymeric nature of the peptide backbone. This structural polymorphism is again more akin to synthetic plastics than proteins.

Wetzel *et al.* also find that the difficulty of inhibiting amyloid aggregation is likely due the ability of amyloid to change packing arrangements without permanent distortions of fibril structure. A small molecule meant to inhibit fibril growth often merely changes the morphology of the final aggregate fiber (reviewed in Wetzel *et al.* 2007). They point out that the presence of nucleating molecules is commonplace in polymer chemistry and that the approach towards small molecule inhibition of aggregation may be a dead end. Instead they suggest an alternative goal of discovering small molecules that change the aggregation pathway to favor non-toxic rather than toxic aggregates.

It seems probable that no single perspective (biochemical analysis, polymer chemistry, or biological adhesion mechanisms) will be universally successful in elucidating questions of amyloid assembly and pathology, and thus all approaches should be considered helpful. It also seems that understanding properties of amyloid fibrils will ultimately prove helpful in advancing aspects of both synthetic and biological adhesion study. For example, in addition to the highly studied pathological influence of amyloid fibrils, it is also known that there are organisms that make use of amyloid fibrils in a functional way. A notable example is *E. coli*, which uses amyloid fibrils (in the form of the protein curlin) to bind to proteins of the host organism, as well as adhere to surfaces on which it will colonize (Chiti and Dobson 2006).

Summary. There are many chemical and physical properties of good bio-adhesive proteins—open conformation with little secondary structure, carbohydrate containing proteins, DOPA containing proteins and heavily modified amino acid sequences with hydroxylation leading to cross-linking, helix formation, fiber-like structure, hydrophobic patches of sequence. Individual biological glues do not exhibit all of these characteristics, but all of them exhibit several different combinations of the above qualities. Common elements among these different characteristics include extensive cross-linking potential (DOPA, carbohydrate groups, hydroxylated amino acids, cysteine residues), and flexible protein conformation or extended structural elements such as β-sheets and fibrils, including amyloid.

A key challenge to using and developing biologically based bonding agents is to attain the same level of bonding power and the variety of useful environments that epoxies, polyurethanes, vinyl polymers, and other polymers can achieve. The rise in popularity of epoxies and other synthetic polymers early on was due primarily to their increase in bonding

power over earlier animal based glues, as well as a greater variety of operating environments and more formulation possibilities.

Primary advantages to the development of adhesive compounds from animal and plant sources is that they represent renewable resources, and that the conditions used for setting or curing these adhesive compounds may be much less harsh than those used for phenolic, vinyl, polyurethane, or epoxy glues. Complete biodegradability (under controllable conditions) while retaining applicable bonding power represents an ultimate goal for environmentally responsible manufacturing of glues. Mild conditions are desirable on multiple levels, particularly that of worker safety and of less potential environmental impact. A selection of biodegradable compounds would be ideal to minimize toxic exposure towards workers and wildlife alike.

The adaptability of organismal systems to environmental conditions is of enormous interest for the development new materials. Also common to biological systems is a largely non-toxic approach to adherents and holdfasts. This is also highly important for a new generation of glues. The ability to lessen or negate the environmental impact and toxicity of industrial glues and compounds is a highly pursued goal among researchers as the human responsibility to preserve the natural world is put increasingly into the forefront by watchdog organizations.

Numerous difficulties stand in the way of novel bio-mimetic materials. These include complex gene control of secreted compounds, difficulty in culturing or harvesting adequate material for study, heavy costs related to extrication of the materials, highly complex extracellular environments, heterogeneity of biological complexes, difficulty in isolating individual system components, and an inability to individually identify specific proteins or glycoproteins and proteoglycans. The difficulties encountered in attempting to analyze current biological systems are prohibitive, and an alternative model is needed. Bio-mimetic materials

cannot be modeled after known biological systems until these systems are understood in enough detail to guide formulation of mimetic compounds.

An alternative model should provide a small enough system to easily study structure/function relationships, and to conveniently manipulate parameters of the proteins under study such as sequence, length, hydrophobicity, cross-linking, glycosylation, and other modifications. Potential glues should be easily obtained in adequate amounts to study. Furthermore, a model system should be easily expandable; that is, new elements should be relatively simple to introduce and examine. This study furthers work done previously on adhesive peptides and works toward establishing a reductionist model that may be used to develop biodegradable peptide-based glues.

Bibliography

Autumn K., M. Sitti, Y.A. Liang, A.M. Peattie, W. Hansen, S. Sponberg, T.W. Kenny, T. Fearing, J.N. Israelachvili, R.J. Full. 2002. Evidence of van der Waals adhesion in gecko setae. Proc. Natl. Acad. Sci. USA. 99, 12252–12256.

Azriel R., E. Gazit. 2001. Analysis of the minimal amyloid-forming fragment of the islet amyloid polypeptide. An experimental support for the key role of the phenylalanine residue in amyloid formation. J Biol. Chem. 276, 34156-34161.

Bechinger C., K.-F. Giebel, M. Schnell, P. Leiderer, H.B. Deising, M. Bastmeyer. 1999. Optical measurements of invasive forces exerted by appressoria of a plant pathogenic fungus. Science. 285, 1896-1899.

Caesar TonThat T.C., L. Epstein. 1991. Adhesion-reduced mutants and the wild type Nectria haematococca: an ultrastructural comparison of the macroconidial walls. Exp. Mcol. 15, 193-205.

Chiti F., C.M. Dobson. 2006. Protein Misfolding, Functional Amyloid, and Human Disease. Annu. Rev. Biochem. 75, 333-366.

Delmonte J. 1989. History of Composites. In: S.M. Lee, editor. Reference Book for Composites Technology. CRC Press, Boca Raton, pp. 1-16.

Epstein L., R.L. Nicholson. 1997. Adhesion of spores and hyphae to plant surfaces In: G. Carroll, P. Tudzynski, editors. The Mycota, vol V. Plant relationships, part A. Springer, Berlin, Heidelberg, New York, pp. 11-25.

Gazit E. 2002. A Possible Role for pi-Stacking in the Self-Assembly of Amyloid Fibrils. FASEB J. 16, 77-83.

Guijarro J.I., M. Sunde, J.A. Jones, I.D. Campbell, C.M. Dobson. 1998. Amyloid fibril formation by an SH3 domain. Proc. Natl. Acad. Sci. USA. 95, 4224–4228.

Haemers S., M.C. van der Leeden, G. Frens. 2005. Coil dimensions of the mussel adhesive protein Mefp-1. Biomaterials. 26, 1231-1236.

Howard R.J., M.A. Ferrari, D.H. Roach, N.P. Money. 1991. Penetration of hard substrates by a fungus employing enormous turgor pressures. Proc. Natl. Acad. Sci. USA. 88, 11281-11284.

Jahn T.R., S.E. Radford. 2008. Folding versus aggregation: Polypeptide conformations on competing pathways. Arch. Biochem. Biophys. 469, 100-117.

Jones M.J., L. Epstein. 1990. Adhesion of macroconidia to the plant surface and virulence of Nectria haematococca. Appl. Environ. Microbiol. 56, 3772-3778.

Kamino K., K. Inoue, T. Maruyma, N. Takamatsu, S. Harayama and Y. Shizuri. 2000. Barnacle cement proteins: importance of disulfide bonds in their insolubility. The J. Biol. Chem. 275, 27360–27365.

Kamino K. 2001. Novel barnacle underwater adhesive protein is a charged amino acid-rich protein constituted by a Cys-rich repetitive sequence. Biochemical Journal. 356, 503–507.

Keimel F.A. 2003. Historical Development of Adhesives and Adhesive Bonding. In: A. Pizzi, K.L. Mittal, editors. Handbook of Adhesive Technology. 2nd ed. CRC Press, Boca Raton, pp. 1-12.

Leblanc C., P. Potin. 2006. Phenolic-based Adhesives of Marine Brown Algae In: A.M. Smith, J.A. Callow, editors. Biological Adhesives. Springer, Berlin Heidelberg, New York, pp. 105-124.

Liu R., C. McAllister, Y. Lyubchenko, M.R. Sierks. 2004. Residues 17-20 and 30-35 of beta-amyloid play critical roles in aggregation. J. Neurosci Res. 75, 162-171.

Monsellier E., F. Chiti. 2007. Prevention of amyloid-like aggregation as a driving force of protein evolution. EMBO Reports. 8 (8), 737-742.

Mostaert A., M. Higgins, T. Fukuma, F. Rindi, S. Jarvis. 2006. Nanoscale Mechanical Characterization of Amyloid Fibrils Discovered in a Natural Adhesive. J. Biol. Phys. 32, 393-401.

Nakano M., Jian-Ren Shen, K. Kamino. 2007. Self-Assembling Peptide Inspired by a Barnacle Underwater Adhesive Protein. Biomacromolecules. 8, 1830-1835.

Naldrett M.J., D.L. Kaplan. 1997. Characterization of barnacle (*Balanus eburneus* and *B. crenatus*) adhesive proteins. Marine Biology. 127, 629–635.

Nielsen L., R. Khurana, A. Coats, S. Frokjaer, J. Brange, S. Vyas, V.N. Uversky, A.L. Fink. 2001. Effect of environmental factors on the kinetics of insulin fibril formation: elucidation of the molecular mechanism. Biochemistry. 40, 6036–6046.

Papov V.V., T.V. Diamond, K. Biemann, J.H. Waite. 1995. Hydroxyarginine-containing polyphenolic proteins in the adhesive plaques of the marine mussel *Mytilus edulis.* J. Biol. Chem. 270, 20183–20192.

Silverman H., F. Roberto. 2007. Understanding Marine Mussel Adhesion. Marine Biotechnology. 9 (6), 661-681.

Stefani M., C.M. Dobson. 2003. Protein aggregation and aggregate toxicity: new insights into protein folding, misfolding diseases and biological evolution. J. Mol. Med. 81, 678–699.

Täljsten, B. 2006. The Importance of Bonding: A Historic Overview and Future Possibilities. Advances in Structural Engineering. 9(6), 721-736.

Tjernberg L., W. Hosia, N. Bark, J. Thyberg, J. Johansson. 2002. Charge attraction and beta propensity are necessary for amyloid fibril formation from tetrapeptides. J. Biol. Chem. 277, 43243-43246.

Uversky V.N., A.L. Fink. 2004. Conformational constraints for amyloid fibrillation: the importance of being unfolded. Biochim. Biophys. Acta. 1698, 131–153.

Waite J.H. 1983. Evidence for a repeating 3,4-dihydroxyphenylalanine-containing and hydroxyproline-containing decapeptide in the adhesive protein of the mussel Mytilus edulis. J Biol. Chem. 258, 2911-2915.

Waite J., X. Qin. 2001. Polyphosphoprotein from the Adhesive Pads of Mytilus edulis. Biochemistry. 40, 2887-2893.

Walker G. Cirripedia. In: F.W. Harrison, A.G. Humes, editors. Microscopic Anatomy of Invertebrates 9: Crustacea, John Wiley 1999, New York, Chichester, pp. 249–311.

Watanabe K., D.G. Parbery, T. Kobayashi, Y. Doi. 2000. Conidial adhesion and germination of Pestalotiopsis neglecta. Mycol. Res. 104, 962-968.

Wetzel R., S. Shivaprasad, A.D. Williams. 2007. Plasticity of amyloid fibrils. Biochemistry. 46 (1), 1-10.

Wiegemann M., B. Watermann. 2003. Peculiarities of barnacle adhesive cured on non-stick surfaces. J. Adhes. Sci. Technol. 17, 1957–1977.

Wiegemann M. 2005. Adhesion in blue mussels (Mytilus edulis) and barnacles (genus Balanus): Mechanisms and technical applications. Aquat. Sci. 67, 166-176.

Winklhofer K.F., J. Tatzelt, C. Haass. 2008. The two faces of protein misfolding: gain- and loss-of-function in neurodegenerative diseases. EMBO J. 27 (2), 336-349.

Xue W.-F., S.W. Homans, S.E. Radford. 2008. Systematic analysis of nucleatio-dependent polymerization reveals new insights into the mechanism of amyloid self-assembly. Proc. Natl. Acad. Sci. USA. 105 (26), 8926-8931.

CHAPTER 2 - Methods and Materials

Materials.

All reagents were ACS certified unless noted otherwise. Phosphotungstic acid (crystalline) was bought from JT Baker (Phillipsburg, NJ). Reagents purchased from Aldrich (Milwaukee, WI) include: 1,2-ethanedithiol, N, N-diisoproplyethylamine, piperidine, and trifluoroacetic acid. Those purchased from Fisher Biotech (Fair Lawn, NJ) were: diethyl ether, N-methylpyrrolidone, dichloromethane, and dimethylformamide. Anaspec, Inc. (San Jose, CA) supplied all protected amino acids. CLEAR-amide resin was bought from Peptide International (Louisville, KY). Cherry wood strips were purchased from Veneer One (Oceanside, NY). Tricholorododecylsilane and trichlorohexadecylsilane were obtained from Fluka (Buchs SG Switzerland). 3-cyanopropyl trichlorosilane was bought from Fisher Scientific (Waltham, MA)

Hydrophobicity measurements.

The Octanol-Interface Scale, which is published on Professor Stephen White's (UC, Irvine) website (http://blanco.biomol.uci.edu/), was used for hydrophobicity values of each amino acid. At pH 12.0 a modified hydrophobicity value for leucine was substituted for lysine's unknown and unpublished value based on physical considerations (Shen 2006, methods). The hydrophobicity value for leucine was modified slightly based on the Henderson-Hasselbach equation for the percentage of lysine present in a charged state at pH 12.0 (Xiaoqun *et al.* 2008, methods). A pKa value of 10.7 was used for the equation for lysine, and resulted in a 5% presence of charged lysines. The accepted value for leucine (-.69 kcal/mol) was weighted

appropriately to reflect the small presence of charged lysines. The final value used for lysine's hydrophobicity (-.57 kcal/mol) was an average of leucine present at 95% and charged lysine (+1.81 kcal/mol) at 5%.

Peptide Synthesis.

Syntheses used an Applied Biosystems Model 431 peptide synthesizer (Foster City, CA). All peptides were synthesized using a 9-fluorenylmethoxycarbonyl (Fmoc) protocol using Fmoc-protected amino acids and CLEAR-amide resin. Resin cleavage was performed with simultaneous deprotection using trifluoracetic acid (95% in water) at room temperature for 2 hours. Cleaved peptides were washed three times with diethyl ether and then dissolved in acetonitrile (20% in water) and lyophilized. All syntheses were characterized by mass spectrometry using a matrix-assisted laser desorption ionization-time of flight (MALDI-TOF/TOF) Bruker Ultraflex II spectrometer (Bruker Daltronics, Billerica, MA).

Preparation for Adhesive Shear Strength Measurement.

Cherry wood was used for shear strength testing and was prepared according to ASTM D2339-98 (Annual Book of ASTM Standards 2002a). A 4% (w/w) solution of peptide in water was stirred for 1 hour at room temperature, then adjusted to pH 12.0 using 1.0 N NaOH. Peptide solutions (360 μL) were spread onto marked 8.0 cm by 2.0 cm areas on one side of two separate strips of wood. The wood strips were allowed to sit for 15 minutes at room temperature, then were pressed together and cured using a Hot Press Model 3890 Auto M (Carver Inc., Wabash, IN). They were pressed for 5 minutes at 130 °C and 1.4 MPa • cm^{-1}. The wood strips were then conditioned for 3 days at 50% relative humidity and 23 °C and subsequently cut into 3 pieces

measuring 2.0 cm x 2.0 cm cured area each. The samples were conditioned again as stated for 4 more days before shear strength measurement.

Adhesive Shear Strength Evaluation.

Shear testing was performed using an Instron Model 4465 (Canton, MA) with a 1.6 mm/min crosshead speed. Stress at maximum load was recorded and averaged across six repeated tests. Wood failure was estimated according to ASTM D5266-99 (Annual Book of ASTM Standards 2002b).

Infrared Spectroscopy.

A 4% (w/w) solution of peptide (100 μL) at pH 12.0 was applied to one side each of two glass microscope slides to an area of 2.0 cm × 2.0 cm. The slides were pressed at 130 °C and 1.4 MPa • cm^{-1} for 5 minutes, then pulled apart by hand and scraped thoroughly with a razor to collect the cured peptide. The collected material was ground with a mortar and pestle. Approximately 0.5 mg of dry peptide was ground with mortar and pestle along with 5 mg KBr pre-dried in an oven, then pressed to 5000 lbs for 5 minutes in a Carver Laboratory Press Model B to produce the pellet. This protocol minimizes interference from water in the 1630-1645 cm^{-1} Amide I region of the spectra. Spectra were recorded on a Nicocent Nexus 670 FT-IR ESP, with values averaged across 16 scans at 2 cm^{-1} resolution, and corrected through background subtraction. The instrument was purged with nitrogen directly prior to every measurement.

Circular Dichroism.

Peptide samples were prepared at different (w/v) concentrations, from a range of 50 μg/mL to 2.8 mg/mL in DI water, or 10 mM NaOH aqueous solution. Assuming 100% weight purity for the dry peptide, the concentrations ranged from (63 μM - 2.0 mM). 2.0 mmol of dried peptide was weighed out (assuming 100% weight purity), and then diluted with the appropriate volume of 10 mM NaOH or DI water. The different test samples corresponded to 2.7 mg AB16 (MW 1363.8 Da), 2.8 mg AB30 (MW 1384.9 Da), and 2.8 mg Islet (MW 1400.9 Da). pH was adjusted by drop-wise addition of 1.0 N NaOH, if required. Peptide solutions were generated with identical (w/v) concentrations in ethylene glycol. Spectra were measured on a J-815 spectrometer (Jasco, Japan) from 260-190 nm using a 1.0 mm path length quartz cuvette. Spectra were averaged over 5 scans. The scan rate was 50 nm/min with a 0.5 nm data pitch at 25 °C. All spectra were corrected by subtracting the background measurement for identical solution without peptide. For the long-term study solutions were stored at room temperature and the spectra were measured every 24 hrs for two weeks. Samples were gently agitated by hand to re-solubilize any settled particles prior to withdrawing aliquots for measurement.

Spectra were recorded in observed ellipticity (θ) with units of mdeg. They were then converted to mean residue ellipticity ([θ]) with units of deg. cm^2 $decimole^{-1}$. This was done with the following equation:

$$[\theta] = \theta / (10\, l\, c\, n)$$

where l is the cuvette pathlength in cm, c is the molar concentration of the peptide assuming 100% weight purity, and n is the number of amino acid residues in the peptide.

Transmission Electron Microscopy.

A stock solution of 10% (w/v) phosphotungstic acid in water was prepared from crystalline phosphotungstic acid. This stock was diluted to 1% for staining samples. 120 microliters of an approximately 1.0 mg/mL water solution of peptide at pH 12.0 was applied to the surface a model 01800-F copper thin bar gridded viewing disc (Ted Pella Inc., Redding, CA) and allowed to stand for 2 minutes. Then the disc was removed with forceps and the solution remaining on top was wicked away with a small strip of Whatman No. 1 filter paper (1 inch square) touched to the side of the disc. The disc was allowed to air dry briefly, then 120 microliters of a 1% solution of phosphotungstic acid solution in water was applied to the top of the disc. This was allowed to sit for 10 minutes, after which the disc was removed and rinsed by allowing several drops of distilled water from a syringe to run down the forceps and over the disc. The disc was then allowed to dry in a closed container. Then the disc was loaded into a Hitachi H-300 transmission electron microscope (Hitachi High Technologies America Inc., Schaumburg, IL) for viewing. Selected representative sections of the sample were photographed with the Hitachi H-300 standard internal camera, using Kodak 4489 standard EM film (Eastman Kodak Company, Rochester, NY) and an exposure time of approximately 3 seconds by hand. The developed photographs were digitized using an HP ScanJet 7400C scanner (Hewlett-Packard Company, Palo Alto, CA) at 1200 dpi.

CHAPTER 3 - Results and Discussion

Background and Previous Studies.

The DHP-sensitive L-type calcium channel is found in human muscle tissue and is involved in calcium linked functions including muscle contraction and neurotransmitter release. This channel interacts with a number of different kinases, including PKA, PKC, and calmodulin-dependent protein kinase. The DHP-sensitive L-type calcium channel also resisted many early attempts at three-dimensional structure determination. In an attempt to elucidate specific motifs involved with formation of an ionic pore in the L-type channel, a previous study involving this laboratory synthesized six predicted transmembrane sequences from the fourth subunit of the channel based on promising primary amino acid sequences (Grove *et al.* 1993). The third predicted transmembrane segment (DPWNVFDFLIVIGSIIDVILSE) synthesized was termed IVS3. These hydrophobic synthetic peptides were inserted into lipid bilayers to ascertain single channel activity. Only two segments, one of them IVS3, formed channels in bilayers. Further study revealed that only the highly hydrophobic IVS3 displayed characteristics of "authentic calcium channels", including differential enantiomer recognition of the DHP derivative BayK 8644 (Grove *et al.* 1993).

The synthesis and purification of IVS3 (Iwamoto *et al.* 1994), displayed some unique properties of the peptide. The sequence is very hydrophobic, as is predicted for most transmembrane sequences. However, after being lyophilized the peptide formed a hard, resilient aggregate that resisted practically every attempt at solvation. It was even somewhat resilient towards physical destruction with a hammer (unpublished observation). The very strong

aggregative propensity indicated possible application as part of a novel *de novo* designed adhesive.

Some years later this laboratory examined a short internal hydrophobic peptide sequence in IVS3 for secondary structure and adhesive capability at various pH values (Shen *et al.* 2006). The original 9-residue core sequence used in the study (FLIVIGSII) was examined with regard to different charged flanking amino acid sequences (ibid.). A second study in which I participated evaluated differences in the sequence length and composition of the hydrophobic core (Xiaoqun *et al.* 2008).

In 2006, Shen *et al.* studied the adhesion properties of various peptide sequences at different pH values. Each peptide consisted of the common hydrophobic IVS3 core sequence FLIVIGSII (h) with different charged amino acid sequences (composed of glutamic acid [E], lysine [K], or the truncated lysine analog 2,3-Diaminopropionic acid [X]) on either side. These flanking sequences yielded differing adhesion strengths dependent on the composition and order of the amino acid sequences, as well as pH. E_3hE_3 proved to be insoluble at low and neutral pH and only weakly adhesive at pH 12.0. K_3hE_3 and E_3hK_3 were mildly adhesive at low and neutral pH conditions, with E_3hK_3 performing slightly better. At high pH E_3hK_3 was significantly superior to K_3hE_3. K_3hK_3 showed the highest adhesive ability at pH 12.0 and X_3hX_3 performed similarly at high pH. Results from Shen *et al.* showed that K_3hK_3 was a random coil at low and neutral pH, while it adopted a β-sheet structure at pH 12.0 along with a very significant increase in adhesion strength. X_3hX_3 adopted a nearly identical CD spectrum.

In the published study by Xiaoqun *et al.* (2008), adhesion was influenced by core length, core sequence, and core hydrophobicity values. Based on the previous study by Shen *et al.*, flanking lysine residues were used for all compounds studied. Table 3-1 shows the sequences prepared for this study.

Peptides	Sequence	MW	pI	ΔG_{avg}(kcal/mol)		
				h_x	pH 7.0	pH 12.0
$K_3h_9K_3$	KKK-FLIVIGSII-KKK	1742.3	10.7	-0.39	0.49	-0.46
$K_3h_{11}K_3$	KKK-VFFLIVIGSII-KKK	1988.6	10.7	-0.43	0.36	-0.48
$K_3h_{12}K_3$	KKK-FLIVIGSIIVIL-KKK	2067.8	10.7	-0.47	0.29	-0.50
$K_3h_7K_3$	KKK-FLIVIGS-KKK	1516.0	10.7	-0.29	0.68	-0.42
$K_3h_{5c}K_3$	KKK-IGSII-KKK	1269.7	10.7	-0.20	0.90	-0.40
$K_3h_{5n}K_3$	KKK-FLIVI-KKK	1371.8	10.7	-0.69	0.67	-0.62
$K_2h_{5c}K_2$	KK-IGSII-KK	1013.3	10.5	-0.20	0.69	-0.31
$K_2h_{5n}K_2$	KK-FLIVI-KK	1115.5	10.5	-0.69	0.42	-0.53
$K_3h_{5mI}K_3$	KKK-IVIGS-KKK	1255.6	10.7	-0.14	0.92	-0.37
$K_3h_{5mL}K_3$	KKK-IVLGS-KKK	1255.6	10.7	-0.11	0.98	-0.36
$K_3h_{5mA}K_3$	KKK-IVAGS-KKK	1213.6	10.7	0.08	1.02	-0.35
KAE_{16}-IV	$(KA)_4(EA)_4$-CO-NH_2	1614.8	6.3	--	1.22	0.62

Table 3-1. Previously synthesized peptides. I synthesized all the five-residue core sequences and the seven-residue sequence as part of my studies. MW – molecular weight, pI – isoelectric point, h_x – mean residue hydrophobicity values (core sequence only), other ΔG_{avg} values – mean residue hydrophobicity of the entire sequence.

I was involved in a large portion of the synthesis and purification for these compounds, synthesizing all the five residue core sequences and the seven-residue sequence. Mean residue hydrophobicity at first appeared to be correlated with increased adhesion strength. However, other than the increase in hydrophobicity between pH 7.0 and pH 12.0, which did show a relationship to increased adhesion strength, there was no correlation between hydrophobicity and adhesion within the two pH groupings as indicated by random distribution of the data within each cluster (Figure 3-1).

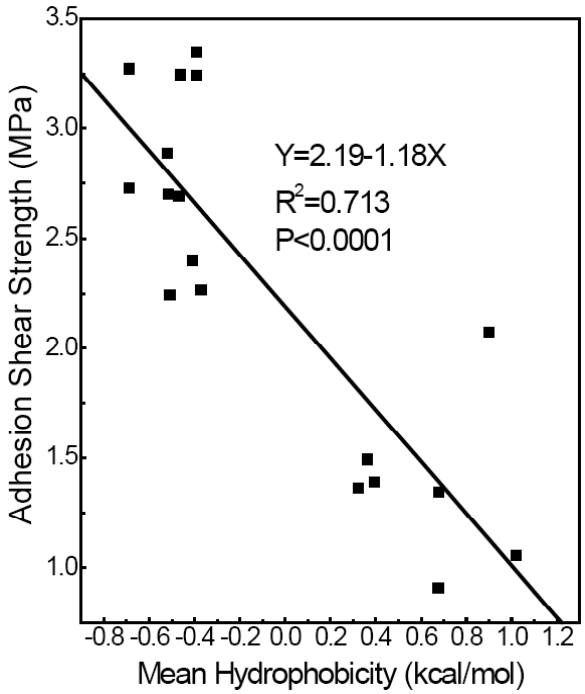

Figure 3-1. Mean residue hydrophobicity as studied in Xiaoqun *et al.* 2008. Adhesion strength vs. hydrophobicity. Values are distributed randomly within each cluster. Clusters are organized around values seen at pH 7.0 and pH 12.0.

The length of the flanking lysine sequence was found to affect adhesion strength, with sequences flanked by two lysyl residues, being measurably weaker than those with three

residues. The length of the core affected adhesion strength, with the $K_3h_5K_3$ sequences superior in strength and the twelve-residue core the weakest. $K_3h_{5n}K_3$ displayed the same ability to form β-sheets as the original nine-residue sequence. Other five residue peptides were unable to form β-structure in water, but did so in ethylene glycol. In addition it was found that a rough, porous wood surface increased adhesion strength over glass slide surfaces, suggesting a mechanical means of glue action whereby the adhesive interlocks with irregularities in the substrate surface. The data suggested that the ability of the core sequence to nucleate further association of monomers into high molecular weight aggregates is important for adhesive qualities. Two of the core sequences examined were picked as analogs to putative amyloid fibril nucleation sites for $A\beta_{1\text{-}40}$ (Xiaoqun *et al.* 2008).

Peptide synthesis, hydrophobicity, and adhesive strength.

Alzheimer's beta amyloid peptide (1-40) has the sequence: DAEFRHDSGYEVHHQ KLVFFAEDVGSNKGAIIGLMVGGVV. For the present study, the putative Aβ nucleation site sequences (Aβ residues 16-21 and 30-35, underlined above) were used in place of previously studied IVS3 hydrophobic cores. Three hydrophobic peptide sequences were synthesized, flanked on each side by lysine residues: KKKLVFFAKKK ($K_2A\beta_{16\text{-}21}K_3$, or $A\beta_{16\text{-}21}$), KKKAIIGLMKKK ($K_3A\beta_{30\text{-}35}K_3$, or $A\beta_{30\text{-}35}$), both from hydrophobic regions of the beta amyloid C-terminus sequence (1-40), as well as KKKIFGAILKKK ($K_3IAPP_{23\text{-}28}K_3$, or $IAPP_{23\text{-}28}$). This third sequence was from the pancreatic islet amyloid polypeptide (IAPP). The aggregation of insoluble IAPP is implicated in type II diabetes mellitus (reviewed in Höppener and Lips 2006). Residues 20-29 of IAPP are thought to serve as the nucleation site for amyloid fibril β-sheet formation (Glenner *et al.* 1988, Azriel and Gazit 2001, Höppener and Lips 2006).

Both $A\beta_{16\text{-}21}$ and $A\beta_{30\text{-}35}$ are fragments of $A\beta_{1\text{-}40}$ originally thought to participate in amyloid nucleation (Murphy 2002). A later study showed that these amyloid residues (16-21 and 30-35) did in fact display an ability to accelerate fibril formation (Liu *et al.* 2004).

The results of peptide synthesis were checked by matrix-assisted laser desorption ionization time-of-flight mass spectrometry (MALDI-TOF/TOF MS). Peaks associated with acetylated and/or sodium-associated products were readily observed, as is common. All three synthetic peptide sequences were readily identified from prominent peaks present in the spectra.

$K_2A\beta_{16\text{-}21}K_3$ (MW 1363.80) displayed single charge (m/z) peaks at 1402.09, 1386.11, 1364.13, 1300.01, 1257.99, and 1171.89 (Figure 3-2). The signal at 1402.09 is representative of the $(M+K)^+$ adduct, while 13.86.11 is the $(M+Na)^+$ product and 1364.13 is the $(M+H)^+$ parent

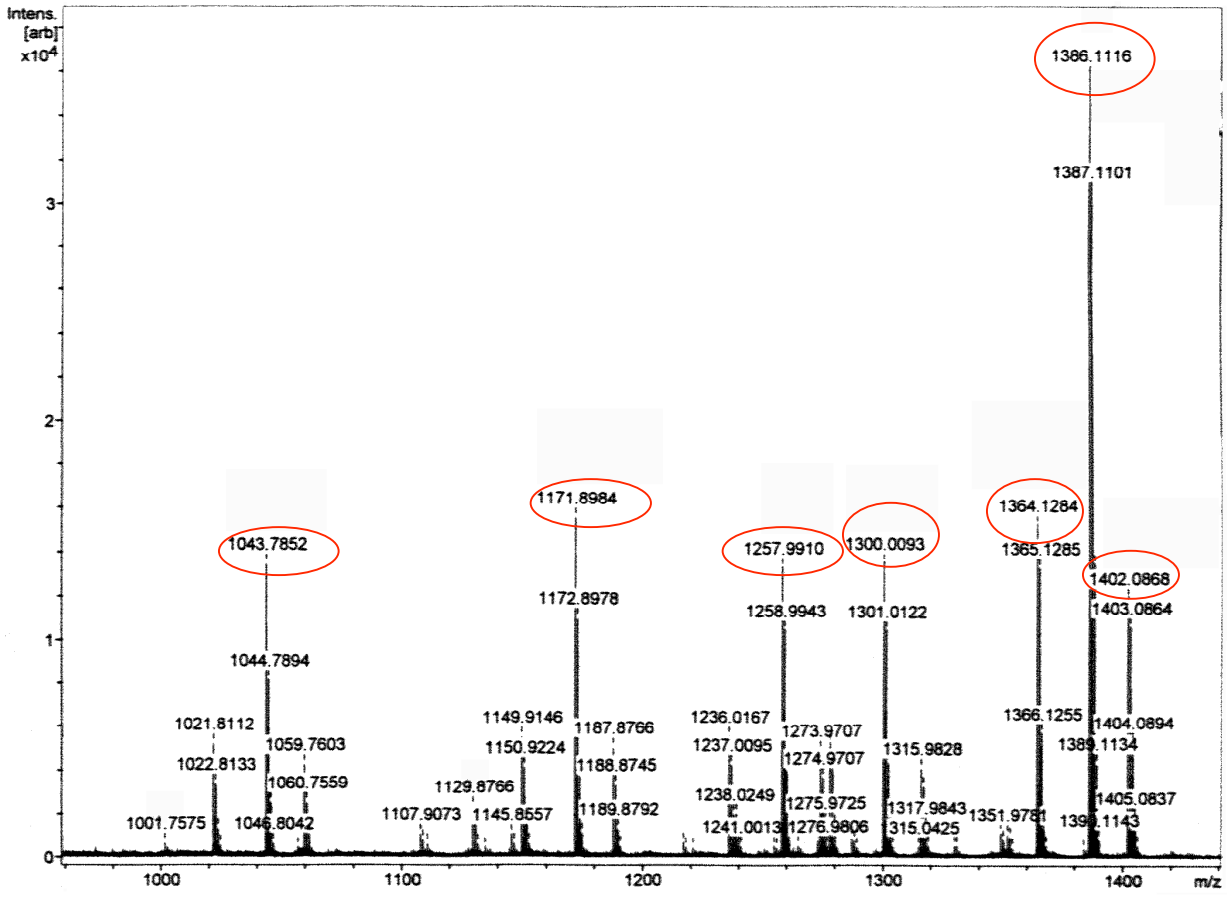

Figure 3-2. $K_2A\beta_{16\text{-}21}K_3$ mass spectrum. Key peaks circled in red.

sequence. 1300.01, 1257.99, and 1171.89 correspond to $(Ac+Na)^+$ products of shortened peptide sequences. These sequences were brought about by progressive losses of lysine tail residues (one, two, or three hydrolyzed residues, respectively). Small peaks were also displayed at 1236.12, 1129.88, 1107.91, and 1001.75. These match the $(M+H)^+$ and $(M+Na)^+$ peaks for abbreviated sequences resulting from the same hydrolyzed lysine residue sequences.

$K_3A\beta_{30\text{-}35}K_3$ (MW 1384.89) displayed characteristic potassium and sodium adduct peaks at 1422.74 and 1406.77, respectively (Figure 3-3). The parent sequence was easily recognized at 1384.78 $(M+H)^+$. Acetylated adducts matching losses of lysine residues were displayed at

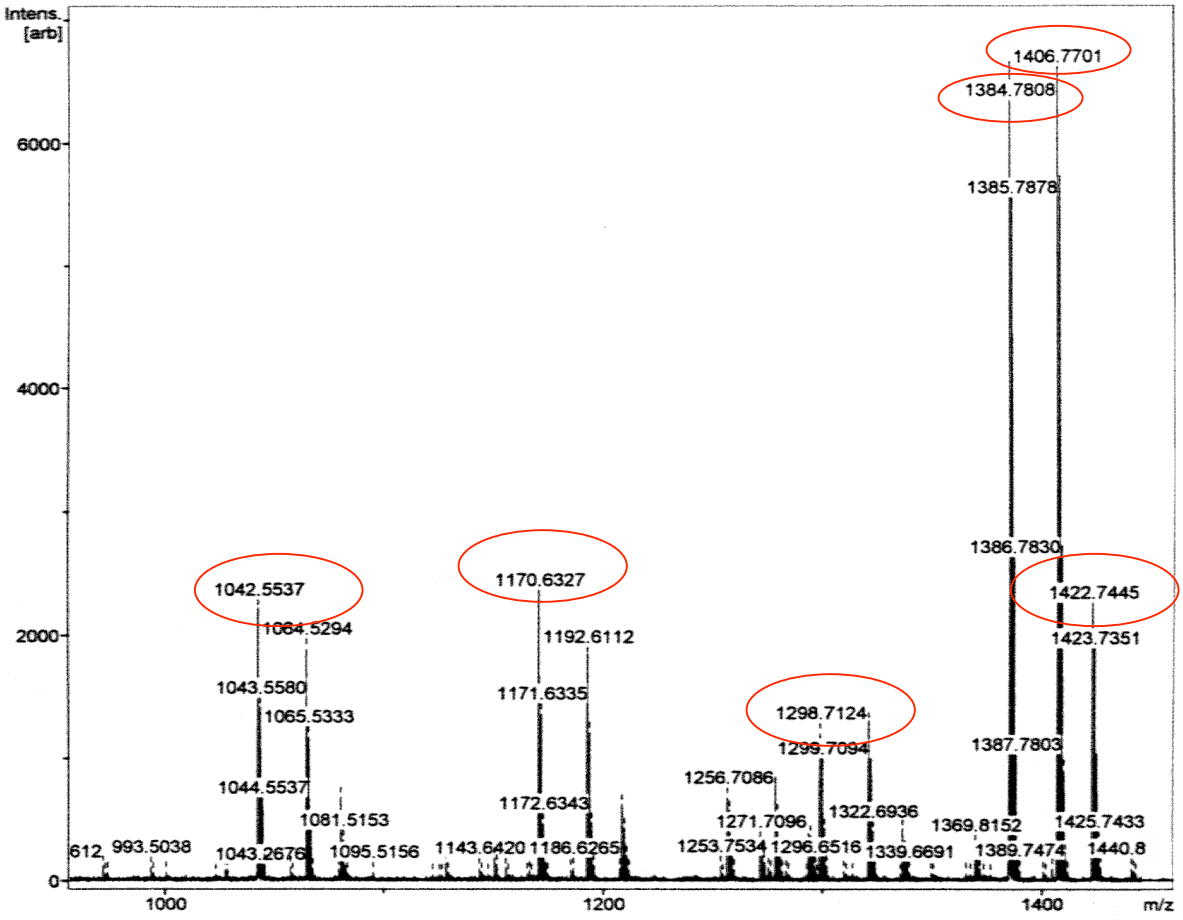

Figure 3-3. $K_3A\beta_{30\text{-}35}K_3$ mass spectrum. Key peaks circled in red.

$K_3A\beta_{30\text{-}35}K_3$ (MW 1384.89) displayed characteristic potassium and sodium adduct peaks at 1422.74 and 1406.77, respectively (Figure 3-3). The parent sequence was easily recognized at 1384.78 $(M+H)^+$. Acetylated adducts matching losses of lysine residues were displayed at 1298.71, 1170.63, and 1042.55. Slightly less intense signals at 1192.61 and 1064.53 correlate to the $(Ac+Na)^+$ adducts of double and triple lysine cleavages. The $(Ac+Na)^+$ product for single lysine hydrolysis was very weak, but present at 1322.69.

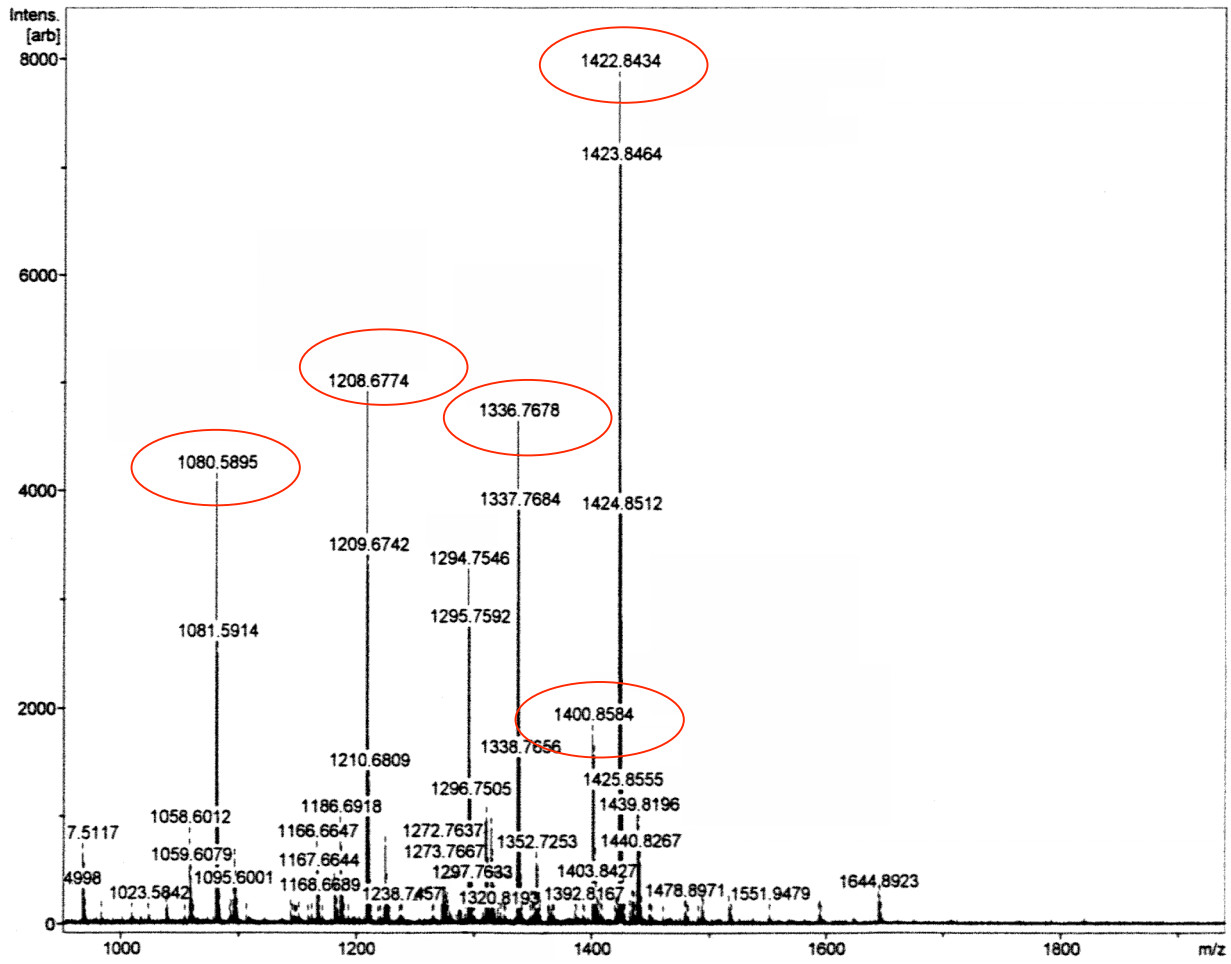

Figure 3-4. $K_3IAPP_{23\text{-}28}K_3$ mass spectrum. Key peaks circled in red.

The spectra for $K_3IAPP_{23-28}K_3$ (MW 1400.87, Figure 3-4) shows a very intense $(M+Na)^+$ peak at 1422.84, with weak $(M+H)^+$ and $(M+K)^+$ signals at 1400.86 and 1439.81. The $(Ac+Na)^+$ adducts of hydrolyzed lysines were dominant at 1336.77, 1208.67, and 1080.59. A moderately intense sodium adduct of single lysine cleavage was seen at 1294.75.

The mean residue hydrophobicity of the core sequences is shown in Table 3-2. The $A\beta_{30-35}$ core sequence AIIGLM had a ΔG_{avg} of -0.21 kcal/mol , with the $IAPP_{23-28}$ core very close at -0.24 kcal/mol. $A\beta_{16-21}$ was twice as hydrophobic with a ΔG_{avg} of -0.41 kcal/mol. All three complete peptides had almost identical positive hydrophobicity values at pH 7.0, and ranged from -0.30 kcal/mol ($IAPP_{23-28}$) to -0.50 ($A\beta_{16-21}$) at pH 12.0. For comparison purposes, $K_3h_{5n}K_3$ (FLIVI) and $K_3h_{5c}K_3$ (IGSII) are also recorded in the table. As previously mentioned, these sequences were analyzed in the last study as analogs to the $A\beta_{16-21}$ and $A\beta_{30-35}$ core sequences, respectively.

					ΔG_{avg} (kcal/mol)	
Peptide	Sequence	MW	pI	h_x	pH 7.0	pH 12.0
$A\beta_{16-21}$	KK-KLVFFA-KKK	1363.8	10.7	-0.41	0.80	-0.50
$A\beta_{30-35}$	KKK-AIIGLM-KKK	1384.9	10.7	-0.21	0.80	-0.39
$IAPP_{23-28}$	KKK-IFGAIL-KKK	1400.9	10.7	-0.24	0.79	-0.30
$K_3h_{5n}K_3$*	KKK-FLIVI-KKK	1371.8	10.7	-0.69	0.67	-0.62
$K_3h_{5c}K_3$*	KKK-IGSII-KKK	1269.7	10.7	-0.20	0.90	-0.40

Table 3-2. Peptide mean hydrophobicity values. MW – molecular weight, pI – isoelectric point, h_x – mean residue hydrophobicity values (core sequence only), other ΔG_{avg} values – mean residue hydrophobicity of the entire sequence. * $K_3h_{5n}K_3$ is included from previous work for comparison as an analog to the $A\beta_{16-21}$ core sequence (Xiaoqun *et al.* 2008). $K_3h_{5c}K_3$ is included from the same work as an analog to the $A\beta_{30-}$

FLIVI displayed more than three times the calculated hydrophobicity of $A\beta_{30-35}$ and $IAPP_{23-28}$ core sequences, as well as the highest whole peptide value (-0.62 kcal/mol) at pH 12.0. As noted in earlier experiments by our lab, the deprotonation of the lysine residues increase the hydrophobicity significantly at pH 12.0. IGSII is nearly identical to the $A\beta_{30-35}$ core: it shows h_x and ΔG_{avg} (pH 12.0) values almost exactly the same to the proposed amyloid nucleation site sequence.

Peptide	Core Sequence	Maximal Adhesive Strength (MPa)
$A\beta_{16-21}$	KLVFFA	3.36 ± .29
$A\beta_{30-35}$	AIIGLM	3.44 ± .12
$IAPP_{23-28}$	IFGAIL	2.89 ± .38
$K_3h_9K_3$°	FLIVIGSII	3.05 ± .35
$K_3h_{5n}K_3$*	FLIVI	3.90 ± .20♦
$K_3h_{5c}K_3$*	IGSII	3.24 ± .13

Table 3-3. Peptide dry adhesive strengths. Samples were tested at 4% (w/v) and hot pressed as described in Methods. ° values from Shen *et al.* 2006. * values from Xiaoqun *et al.* 2008. ♦ Maximal adhesion strength occurs at 2% (w/v).

These hydrophobic core sequences were tested for dry heat-pressed adhesive strength at pH 12.0 (Table 3-2 and Figure 3-5). Two previously studied peptides ($K_3h_{5n}K_3$ and $K_3h_{5c}K_3$) are included for comparison. Testing was done at a 4% (w/v) solution, which had been indicated as the concentration of $K_3h_9K_3$ that gave maximal adhesion strength (Shen *et al.* 2006). $K_3h_{5n}K_3$ was an exception and was tested at 2% (w/v) based on results obtained in earlier work (Xiaoqun *et al.* 2008). Corresponding to the high mean hydrophobicity at pH 12.0, the dry adhesion

strength of $K_3h_{5n}K_3$ was also higher than any of the three tested peptides, with $IAPP_{23-28}$ being the weakest. Shear strength for the peptides $A\beta_{16-21}$ and $A\beta_{30-35}$ was similar at 3.36 and 3.44 MPa, respectively. In addition, the analog sequence $K_3h_{5c}K_3$ demonstrated dry adhesive strength slightly higher than $A\beta_{30-35}$ (3.24 MPa). $IAPP_{23-28}$ showed weaker adhesion strength at 2.89 MPa.

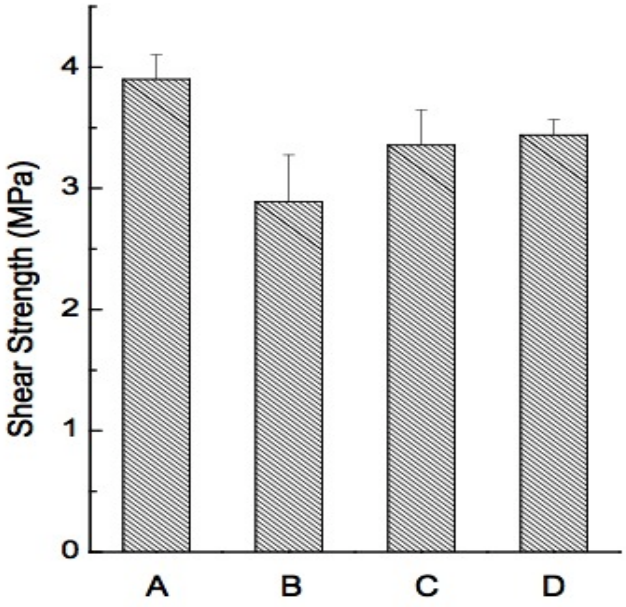

Figure 3-5. Dry adhesive shear strengths. Column A represents peptide $K_3h_{5n}K_3$ from previous work (Xiaoqun *et al.* 2008). B represents the sequence $IAPP_{23-28}$. Column C is the amyloid sequence $A\beta_{16-21}$, and column D is $A\beta_{30-35}$. All four peptides show roughly similar adhesion strengths, but only $K_3h_{5n}K_3$ forms beta structure without being heat-pressed. $K_3h_{5c}K_3$ shear strength value not shown.

Circular dichroism studies.

In our previous work with these hydrophobic sequences it was determined that many of the peptides formed regular secondary structure in solution. It was hypothesized that ordering of the peptides into β-structure was important factor for adhesion strength (Shen *et al.* 2006, Xiaoqun *et al.* 2008). From this work, sequences $K_3h_{5n}K_3$ formed β-sheets in aqueous solution at

pH 12.0, and while others ($K_3h_{5c}K_3$, $K_3h_{5ml}K_3$) remained disordered regardless of pH, most likely as a result of water molecules successfully competing for structural hydrogen bond sites. They formed secondary elements only in the absence of water (i.e. ethylene glycol as a solvent).

Further testing was performed to ascertain what affect the small amount of partially charged lysine had on β-sheet formation (Xiaoqun *et al.* 2008). This was done using ethylene glycol as the solvent, where deprotonation of lysyl residues could not occur. $K_3h_{5n}K_3$ and another sequence from the middle of FLIVISGSII ($K_3h_{ml}K_3$) were dissolved in ethylene glycol and CD spectra were recorded. Both peptides remained randomly structured. When the remaining lysyl charges were removed by re-synthesizing the peptides with formylated lysine residues β-structure was easily formed in the absence of water (Figure 3-6).

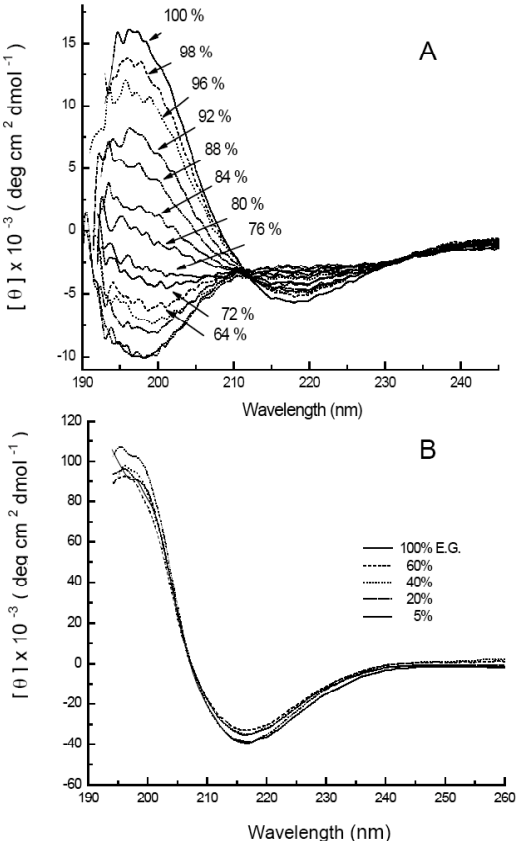

Figure 3-6. Effect of lysine charge removal on β-structure. Figure from Xiaoqun *et al.* 2008. **A.** The presence of water affects β-sheet formation by $K_3h_{ml}K_3$. Percentage of ethylene glycol is indicated with arrows. **B.** $K_3h_{5n}K_3$ shows no change.

Removal of remaining charges on the lysine residues removes repulsive charge-charge interactions and thus increases the peptides' ability to form β-sheets. Both alkaline pH and substitution of lysine residues with formylated analogs accomplish the same thing and hence both lead to β-structure formation. When water is introduced to the solution it competes for hydrogen bonding, which results in a decrease in β-structure (Figure 3-6A). However this effect is dependent on the ease with which water can access the hydrogen bond interactions. $K_3h_{5n}K_3$ does not show a decrease in β-structure with addition of water (Figure 3-6B), suggesting its network of hydrogen bonds is less accessible to water than that of $K_3h_{mI}K_3$.

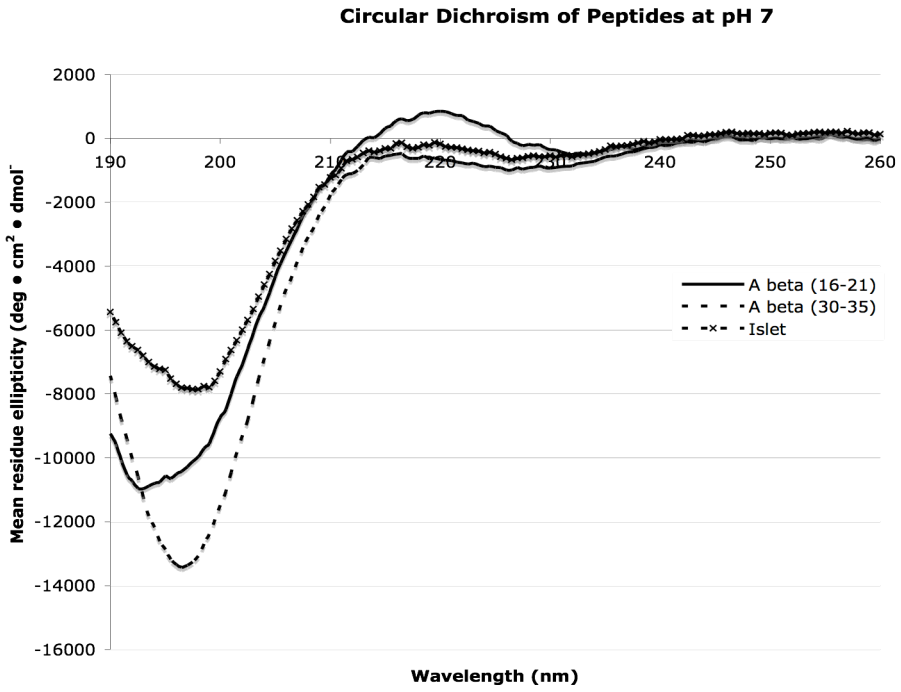

Figure. 3-7. Circular dichroism at pH 7.0. Data for 125 μM peptides. Figure is representative of all peptide spectra at all concentrations. All three sequences are unstructured in water at pH 7.0.

Based on the similarity between $K_3h_{5n}K_3$ and $K_3h_{5c}K_3$ to $A\beta_{16-21}$ and $A\beta_{30-35}$, respectively, we investigated the ability of $A\beta_{16-21}$, $A\beta_{30-35}$, and the $IAPP_{23-28}$ sequences to form regular β-

structure in different solvent systems. None of the peptides formed regularly ordered structure in neutral aqueous solution (Figure 3-7) at any concentration tested (63 μM to 2.0 mM), with signal noise increasing rapidly at higher concentrations. At pH 12.0, $A\beta_{16-21}$ displayed an unusual spectral shape with a maximum at 204 nm and minimum at 228 nm (Figure 3-8). However, this does not match any peak minimum or maximum for α helical or β-structure. This same shape appeared at all tested concentrations at pH 12.0. Both $A\beta_{30-35}$ and $IAPP_{23-28}$ peptides remained randomly structured across the range of concentrations under these conditions as well. Solutions in ethylene glycol were created to determine if the absence of competition from water would facilitate intermolecular hydrogen bond formation (Figure 3-9). These runs also showed only randomly structured spectra for all samples.

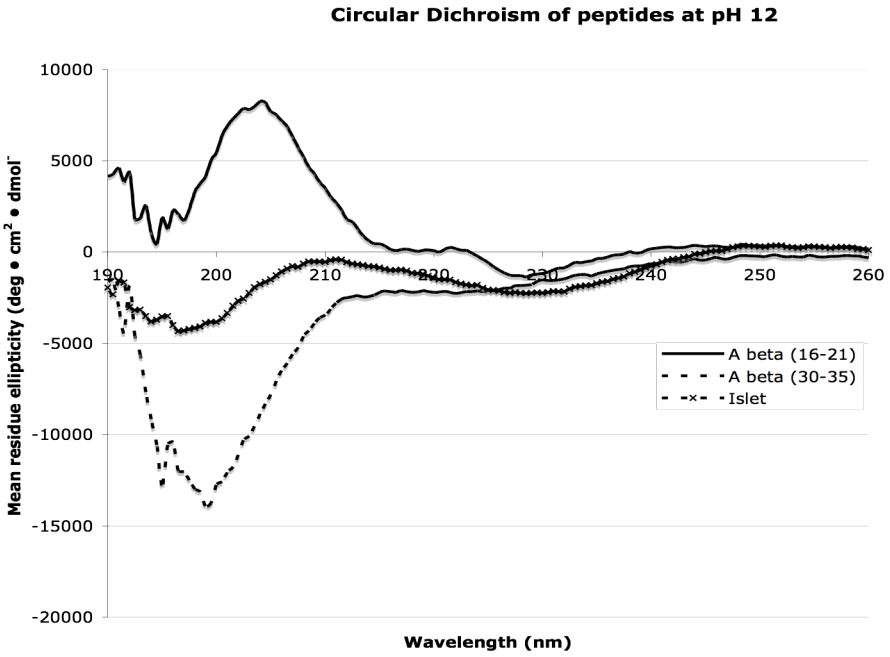

Figure 3-8. Circular dichroism at pH 12.0. Data for 125 μM peptides. Figure is representative of all samples at all concentrations. $A\beta_{16-21}$ forms an unusual spectrum, but does not match with any known peak minimum or maximum for α- or β-structure. $A\beta_{30-35}$ and $IAPP_{23-28}$ are randomly structured. These signals remained the same for each sample throughout a two week period of daily measurement.

Previously it had been determined that the formation of β-sheets in solution by $A\beta_{1-40}$ could take up to several days (unpublished data by Takeo Iwamoto). Therefore, to test if secondary elements would develop over time, CD spectra were taken daily for two weeks in both solvent systems. This analysis showed no secondary structure either, with $A\beta_{16-21}$ forming its unusual spectrum for all measurements (data not shown). Thus there appears to be no regular structural component to the solution, in contrast to earlier experiments. However, as there was clearly a glue-like function to the peptides and earlier sequences had shown a preservation of β-structure with dry hot-pressing (Shen *et al.* 2006, Xiaoqun *et al.* 2008), it was thought likely that secondary structure was generated only during the dry hot-pressing protocol associated with the shear strength assays.

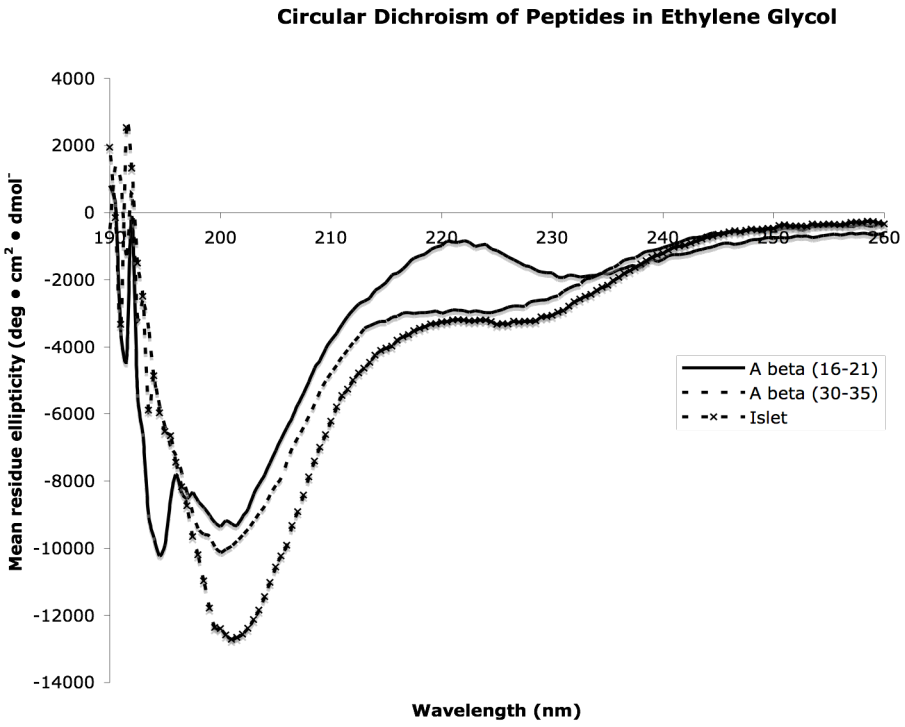

Figure 3-9. Circular dichroism in ethylene glycol. Data for 125 μM samples. Figure is representative of all concentrations. All samples are random coil.

FT-IR Measurements.

To determine if β-sheet formation was indeed dependent on the hot pressing action, Solid state FT-IR was performed on samples of each peptide that had been heated and pressed on glass slides at 130 ºC. By far, the most widely used infrared region for determining secondary elements is the Amide I region, which is primarily due to C=O stretching on the main chain. This region produces peaks generally clustered between 1630 cm^{-1} and 1643 cm^{-1} for native β-sheets, and is shifted slightly lower by the presence of amyloid β-structure to 1611-1630 cm^{-1} (Zandomeneghi *et al.* 2004).

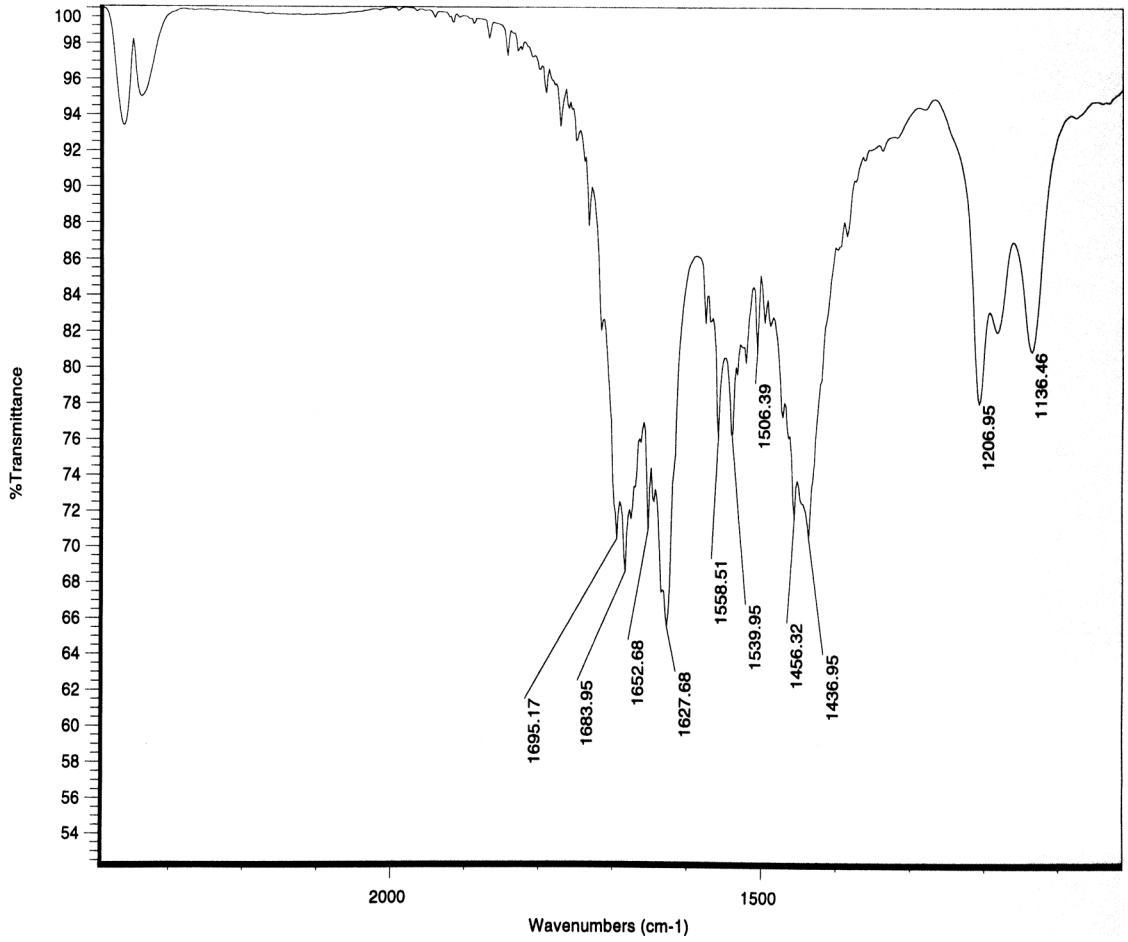

Figure 3-10. $A\beta_{16-21}$ Infrared spectrum. Sample shows peaks in the Amide I band at 1627 cm^{-1} and 1684 cm^{-1}, and the Amide II band at 1558 cm^{-1} and 1540 cm^{-1}. This indicates β-sheet structure, possibly anti-parallel sheet due to the peak at 1684 cm^{-1}.

All three sequences showed the characteristic peaks for β-structure, with Amide I peaks at 1627 cm^{-1}, 1629 cm^{-1}, and 1633 cm^{-1} for $A\beta_{16-21}$, $IAPP_{23-28}$, and $A\beta_{30-35}$, respectively (Figures 3-10 through 3-12). These peaks are on the upper portion of the amyloid-shifted Amide I region and clearly show β-sheet conformation. All three compounds also contain a less intense peak at 1684 cm^{-1}, which is present in proteins containing anti-parallel β-sheets, and is generally characteristic of the conformation. In addition, the spectra support the idea that these synthetic peptides may aggregate into a supramolecular structure similar to amyloid fibrils when in the adhesive state. Amide II peaks were also present in all three samples at 1558 cm^{-1} and 1540 cm^{-1} (Figures 3-10 through 3-12).

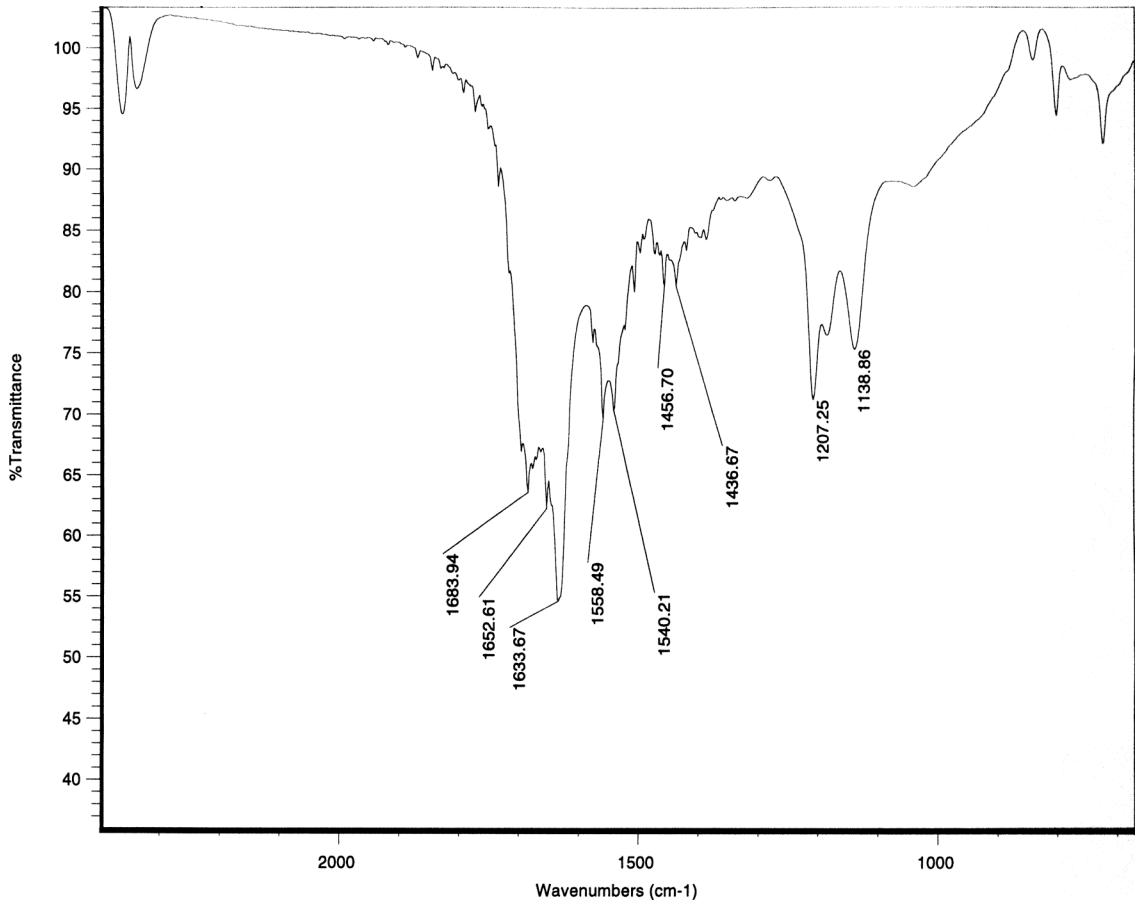

Figure 3-11. $A\beta_{30-35}$ infrared spectrum. Sample shows peaks in the Amide I band at 1633 cm^{-1} and 1684 cm^{-1}, and the Amide II band at 1558 cm^{-1} and 1540 cm^{-1}.

These results indicate that although there are no secondary elements in solution, the hot pressing action forms regular β-structure in the cured adhesive. Thus, these data present a third category of adhesive. From our earlier studies we discerned two classes—adhesives that formed regular β-structure in water (FLIVIGSII, FLIVI), and those that required water to be absent for β-sheet formation (IGSII, IVIGS). In these prior two categories, the β character was preserved with desiccation and curing for wood shear tests. Now we have confirmed another category—a class of peptides that requires hot-pressed curing to form secondary structure and assemble into a high-molecular weight bonding agent.

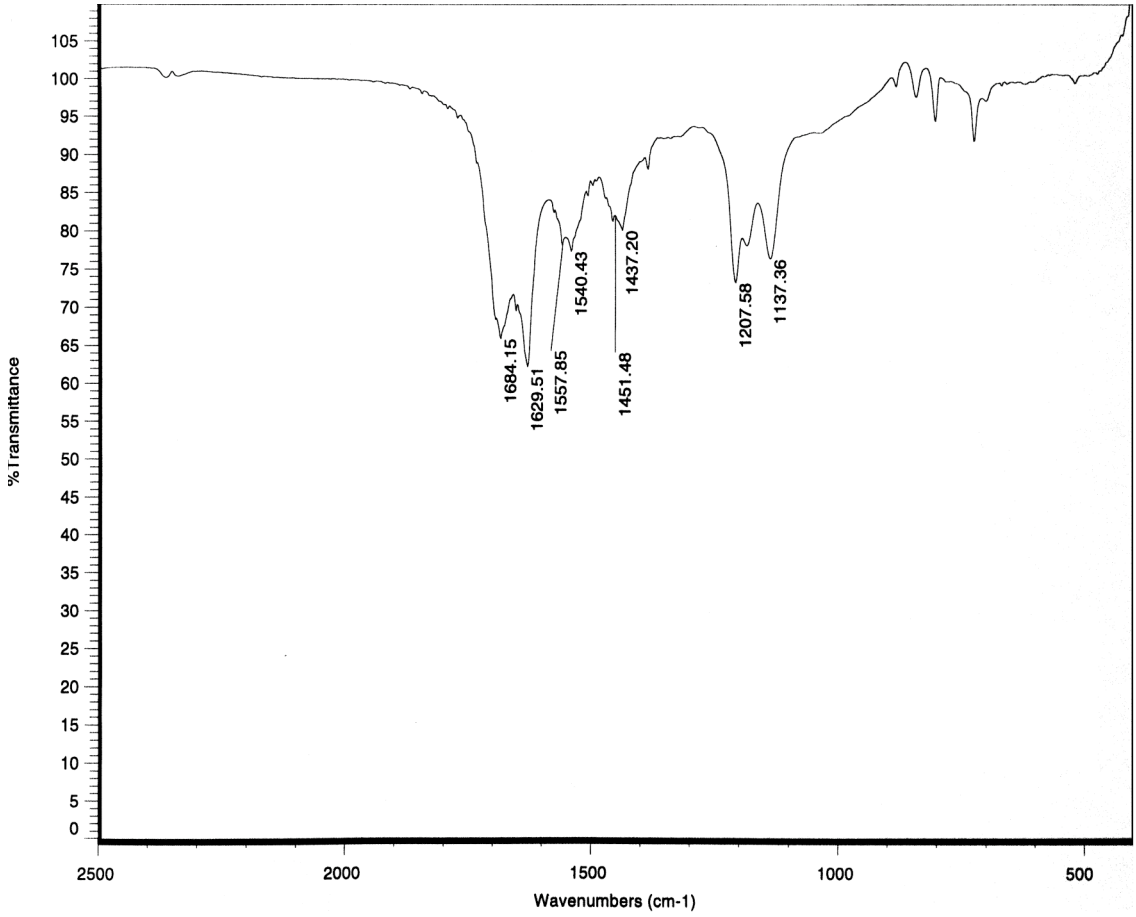

Figure 3-12. $IAPP_{23-28}$ infrared spectrum. Sample shows peaks in the Amide I band at 1629 $cm^{-1}$and 1684 cm^{-1}, and the Amide II band at 1558 cm^{-1} and 1540 cm^{-1}.

Transmission Electron Microscopy.

Because these adhesives are thought to work through mechanical means (Shen *et al.* 2006, Xiaoqun *et al.* 2008), and because the dried compounds displayed β-sheet structure with a possible amyloid signature, Transmission electron microscopy was performed to determine if there was a fibrillar morphology to the dried peptide glues. $A\beta_{16\text{-}21}$ and $A\beta_{30\text{-}35}$ had previously been shown to nucleate amyloid fibril formation (Liu *et al.* 2004). Therefore $K_3h_{5n}K_3$ was examined, as it contained an analogous sequence and similar hydrophobicity to the nucleation sequence $A\beta_{16\text{-}21}$ and had already been determined to assume a β-sheet conformation in aqueous solution.

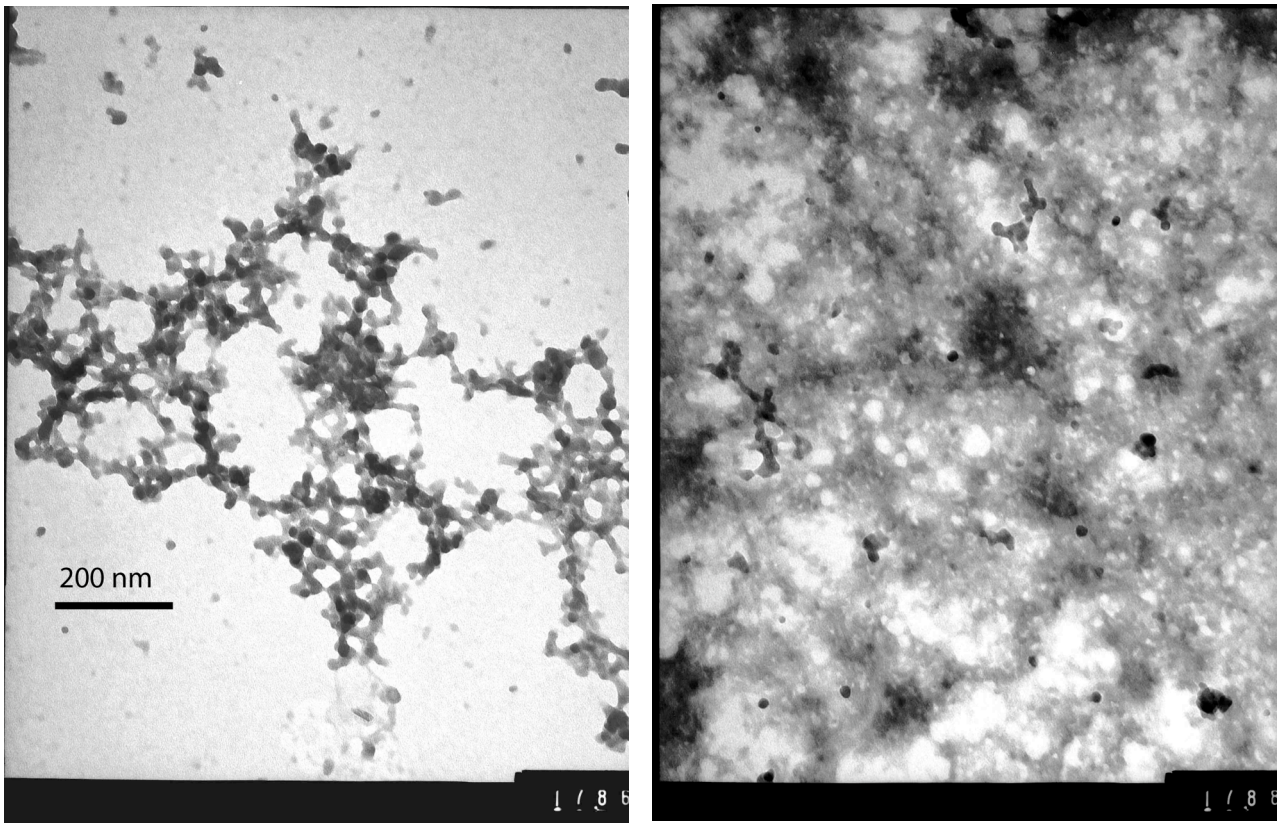

Figure 3-13. Transmission electron micrograph of $K_3h_{5n}K_3$ at pH 7.0 and 70,000x. **A**. Left, the peptide adopts an extended globular superstructure in a thin and irregular network. **B**. Right, thick aggregate, still globular and spongy.

At pH 7.0 TEM images showed a thin and irregular globular meshwork (Figure 3-13a). In areas of higher concentration a thick aggregate was formed (Figure 3-13b), but the spongy, globular structure remained. No amyloid-like structures were detected. This supports the data indicating that the peptide must be at alkaline pH in order to perform as a glue. The globular nature of the peptide is roughly similar to electron micrographs of barnacle cement (Wiegemann 2005, Figure 5a), though much more disordered and far less uniform than the barnacle matrix. When recorded at pH 12.0, micrographs demonstrated that $K_3h_{5n}K_3$ had undergone a conformational change to a fibrous structure (Figure 3-14a,b). Comparison with beta amyloid fibrils (Figure 3-15) shows a similar morphology, though the peptide protofibrils have a less regular shape than the Aβ fibrils.

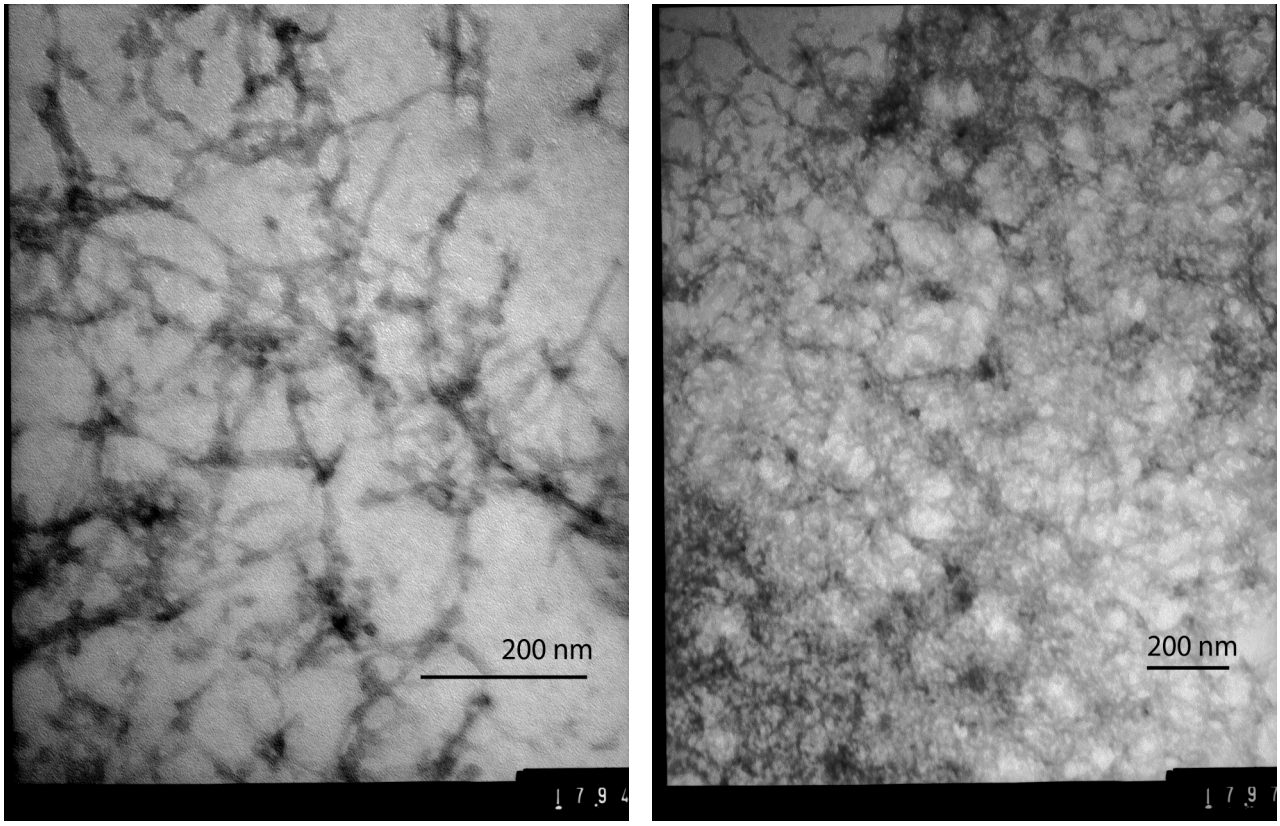

Figure 3-14. TEM of $K_3h_{5n}K_3$ at pH 12.0. **A.** Left, the peptide adopts a fibrous morphology in the adhesive state (100,000x). **B**. Right, thicker aggregation still displays a fibrillar structure (50,000x). Compare with pH 7 micrographs.

Earlier studies had discovered that while small peptide sequences displayed significant bonding power with a wooden shear strength test, changing the substrate to sialyated glass microscope slides eliminated all glue strength (Xiaoqun *et al.* 2008). Glass sialyation eliminates surface irregularities and ensures that the glass is uniformly hydrophobic. If adhesion were due significantly to hydrophobic interactions at the glue-substrate interface, this test would reveal the retention of some adhesive strength. However, peptides were completely unable to bond the two slides. Consequently a mechanical mechanism for bonding power was proposed, whereby small pores and crevices provide anchor points for the nanomaterial to interlock with the substrate. These current results clearly validate the hypothesis proposed in previous studies that adhesive quality is mechanical in nature and is due to the formation of a fibrous superstructure that entangles and interlocks with deformations on the substrate surface.

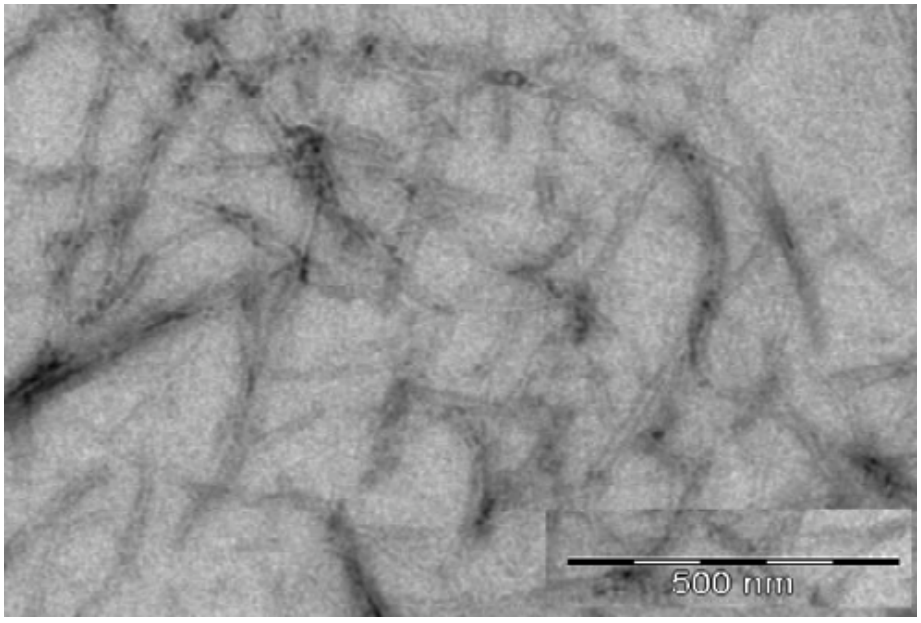

Figure 3-15. TEM of Aβ fibrils. Figure from Khan *et al.* 2005. Comparison with Figure 9 shows marked differences at pH 7. However, $K_3h_{5n}K_3$ displays similar fibril structure in the adhesive state (Figure 14).

CHAPTER 4 - Conclusions

Core Sequence	FLIVIGSII, FLIVI	IVIGS, IGSII	IFGAIL, KLVFF, AIIGLM
Low pH	Random	Random	Random
Neutral pH	Random	Random	Random
High pH, Water Solvent	β-structure	Random	Random
High pH, Organic Solvent (ethylene glycol)	β-structure	β-structure	Random
High molecular weight in water solvent	Yes, greater than 10^6 Da	No	No
Drying effect on Structure	β-structure preserved	β-structure preserved	β-structure only when heated and pressed
Adhesion Strength	Good	Good	Good
Adhesive Super-Structure	Fibril –previously unknown	Unknown	Fibril

Table 4-4. Summary of core sequence properties studied to date. The present study establishes a third category among studied hydrophobic core peptides (right most column). This category will not form regular secondary elements in solution and requires heated dry pressing to form β-structure.

Summary of Results.

Previously we had reported work with other short peptides exhibiting adhesive characteristics (Shen *et al.* 2006, Xiaoqun *et al.* 2008). These current peptides show similar propensities. We now have three classes of peptides that show adhesive qualities: peptides

which will become structured in the presence of water, peptides that assemble only in the absence of water, and peptides that will assemble only when heat-pressed and cured. The properties of each class are summarized in Table 4-4. This assembly is what leads to the mechanical means of adhesion seen with these peptides. The three sequences used for the hydrophobic core peptides were previously reported nucleation regions for amyloid aggregation, and all three original sequences showed the ability to accelerate pathological aggregation in their parent polypeptides (Azriel and Gazit 2001, Liu *et al.* 2004).

Tables 3-1 and 3-2 detail hydrophobicity for past and present sequences, and Table 3-3 shows shear strength values. $A\beta_{16\text{-}21}$ contained the most hydrophobic core at -0.41 kcal/mol, with $A\beta_{30\text{-}35}$ and $IAPP_{23\text{-}28}$ very near at -0.21 and -0.24 kcal/mol, respectively. The previously studied analog sequence FLIVI was significantly more hydrophobic than $A\beta_{16\text{-}21}$, while $K_3h_{5c}K_3$ was almost identical to $A\beta_{30\text{-}35}$ in core hydrophobicity and whole peptide hydrophobicity at both neutral and alkaline pH. Adhesive strength was highest in $A\beta_{30\text{-}35}$ at 3.44 MPa, although not statistically significant from $A\beta_{16\text{-}21}$. Both the amyloid sequences were similar in dry strength to their previously studied analogs, $K_3h_{5n}K_3$ and $K_3h_{5c}K_3$. $IAPP_{23\text{-}28}$ was significantly weaker at 2.89 MPa, which suggests that the core sequence cannot hydrogen bond as effectively as the other samples in β-sheets.

Even though CD determined that both $K_3h_{5n}K_3$ and the original sequence (FLIVIGSII) readily formed secondary elements when the flanking lysines were uncharged, the peptides for the three nucleation sites did not form any discernible periodic structure in aqueous solution. $A\beta_{30\text{-}35}$ and $IAPP_{23\text{-}28}$ were random coils at both neutral and alkaline pH. $A\beta_{16\text{-}21}$ altered conformation with pH, however this change did not reveal any regular structural elements. Instead $A\beta_{16\text{-}21}$ formed an unusual spectra whose peaks matched no known values for regular

secondary structures with a maximum at 204 nm and minimum at 228 nm. This was the only evidence of structure observed in any solvent by any of the peptides (Figures 3-7 through 3-9). In ethylene glycol all three samples remained random across all concentrations tested.

Infrared spectroscopy revealed that heat-pressing and curing the peptides generated a clear β-sheet structure for each of the amyloid nucleating sequences (Figures 3-10 through 3-12). It appears that the heat with pressure curing is necessary for the formation of secondary stuctural elements and enhanced adhesion strength. In peptides that assembled in solution, β-structure was preserved during the curing process. Thus it appears the formation of β-sheets in a desiccated state is a requirement for performance. These peptides appear to represent a new class of nanomaterials that do not undergo amyloid-like aggregation until desiccated. Once dried, however, all sequences showed structure in agreement with earlier experiments (Xiaoqun *et al.* 2008), including a peak at 1684 cm^{-1} that is characteristic of the presence of anti-parallel β-sheets. Amide I and II band peaks were present in all samples. $A\beta_{16-21}$ showed peaks at 1627 cm^{-1}, 1558 cm^{-1}, and 1540 cm^{-1}. $A\beta_{30-35}$ and $IAPP_{23-28}$ samples recorded peaks practically the same, with slight variations (Amide I peaks at 1633 cm^{-1} and 1629 cm^{-1}, respectively).

Transmission electron microscopy (Figures 3-13 and 3-14) showed fibrils present at pH 12.0 for $K_3h_{5n}K_3$. A kind of loose, irregular network of globular mesh was present at neutral pH, transitioning into a sponge-like aggregate in areas of high sample concentration. The overall morphology was roughly akin to that of barnacle cement samples (Wiegemann 2005, Figure 5a), but much less uniform and less ordered. Elevated pH brought about a transformation to fibrils with characteristics similar to Aβ samples (Figure 3-14). These results lend more support to the hypothesis that the small peptide-based nanomaterials under study form protofibrils in the glue

state. These protofibrils are the structural means by which mechanical interlocking and entanglement of the substrate is achieved.

Future directions.

In order for the synthesis of peptide-based nanomaterials to be commercially viable, the properties governing the assembly and manipulation of bio-mimetics must be elucidated. This is much more easily done in a reductionist approach using short peptide fragments that can be easily made and studied. The numerous difficulties associated with the study of biological glues in the context of their natural manufacture are prohibitive to ascertaining how to manipulate and control the various qualities needed to make bio-based materials widely applicable. Instead of dealing with complex extracellular environments and complicated purification methods in an effort to isolate proteins for further study, a reductionist model such as the one used here allows researchers to concentrate on understanding how interplay between various intermolecular forces affect the performance of nanomaterials. This in turn allows a quicker progression towards manipulating these characteristics toward research goals such as biodegradable, non-toxic materials useable in an industrial or medical setting.

Further studies into the properties and conditions controlling self-assembly and adhesion are necessary. Future goals should include the study of various cross-linking methods for the improvement of glue function, fine-tuning manipulation of peptide structure and assembly through specific environmental manipulation, and possible structural modifications to the synthetic peptides such as branching structure or linking different core sequences in order to increase the effectiveness of mechanical entanglement. Priority should be given to non-covalent mechanisms in order to optimize a peptide structure that is likely to be even more effective when

cross-linking is finally introduced. It is very important that the three-dimensional structure of the adhesive state be illuminated, as this would give a huge boost to the rational design of new peptides and sequence modifications in addition to accelerating the detailed understanding of the specific mechanisms leading to effective design.

Ultimate applications of biologically based adhesives could include completely biodegradable surgical thread, bandages, and other materials that could potentially decrease healing time and scarring in surgery patients or the chronically ill. Leaving aside glue-specific research, understanding how to manipulate peptide-based materials could lead to novel drug delivery methods or tissue engineering through an ability to manipulate scaffolding structures at the nanoscale level.

Bibliography

Annual Book of ASTM Standards, Standard Test Method for Strength Properties of Adhesive in Two-Ply Wood Construction in Shear by Tension Loading. D2339-98, American Society for Testing and Materials: PA, 2002, Vol. 15.06, pp. 158-160.

Annual Book of ASTM Standards, Standard Practice for Estimating the Percentage of Wood Failure in Adhesive Bonded Joints. D5266-99, American Society for Testing and Materials: PA, 2002, Vol. 15.06, pp. 443-446.

Azriel R., E. Gazit. 2001. Analysis of the minimal amyloid-forming fragment of the Islet amyloid polypeptide. An experimental support for the key role of the phenylalanine residue in amyloid formation. J Biol. Chem. 276, 34156-34161.

Glenner G.G., E.D. Eanes, C.A. Wiley. 1988. Amyloid fibrils formed from a segment of the pancreatic islet amyloid protein. Biochem. Biophys. Res. Commun. 155, 608-614.

Grove A., J.M. Tomich, T. Iwamoto, M. Montal. 1993. Design of a functional calcium channel protein: Inferences about an ion channel-forming motif derived from the primary structure of voltage-gated calcium channels. Protein Sci. 2, 1918-1930.

Höppener J.W., C.J. Lips. 2006. Role of islet amyloid in type 2 diabetes mellitus. Int. J. Biochem. Cell Biol. 38 (5-6), 726-736.

Iwamoto T., A. Grove, M.O. Montal, M. Montal, J.M. Tomich. 1994. Chemical synthesis and characterization of peptides and oligomeric proteins designed to form transmembrane ion channels. Int. J. Pept. Protein Res. 43 (6), 597-607.

Khan A., A.E. Ashcroft, V. Higenell, O.V. Korchazhkina, C. Exley. 2005. Metals accelerate the formation and direct the structure of amyloid fibrils of NAC. J. Inorg. Biochem. 99, 1920-1927.

Liu R., C. McAllister, Y. Lyubchenko, M.R. Sierks. 2004. Residues 17-20 and 30-35 of beta-amyloid play critical roles in aggregation. J Neurosci. Res. 75, 162-171.

Murphy R.M. 2002. Peptide Aggregation in Neurodegenerative Disease. Annu. Rev. Biomed. Eng. 4, 155-174.

Shen X.C., X.Q. Mo, R. Moore, S.J. Frazier, T. Iwamoto, J.M. Tomich, X.Z. Sun. 2006. Novel pH dependent adhesive peptides. J. Nanosci. Nanotechnol. 6, 837-844.

Wiegemann M. 2005. Adhesion in blue mussels (Mytilus edulis) and barnacles (genus Balanus): Mechanisms and technical applications. Aquat. Sci. 67, 166-176.

Xiaoqun M., Y. Hiromasa, M. Warner, A.N. Al-Rawi, T. Iwamoto, T.S. Rahman, X.Z. Sun, J.M. Tomich. 2008. Design of 11-Residue Peptides with Unusual Biophysical Properties: Induced Secondary Structure in the Absence of Water. Biophys. J. 94, 1807-1817.

Zandomeneghi G., M.R.H. Krebs, M.G. McCammon, M. Fändrich. 2004. FTIR reveals structural differences between native β-sheet proteins and amyloid fibrils. Protein Science. 13, 3314-3321.